How to cite: *Angew. Chem. Int. Ed.* **2024**, *63*, e202316364
doi.org/10.1002/anie.202316364

London Dispersion

Advances and Prospects in Understanding London Dispersion Interactions in Molecular Chemistry

*Lars Rummel and Peter R. Schreiner**

Dedicated to Kendall N. Houk on the occasion of his 80th birthday.

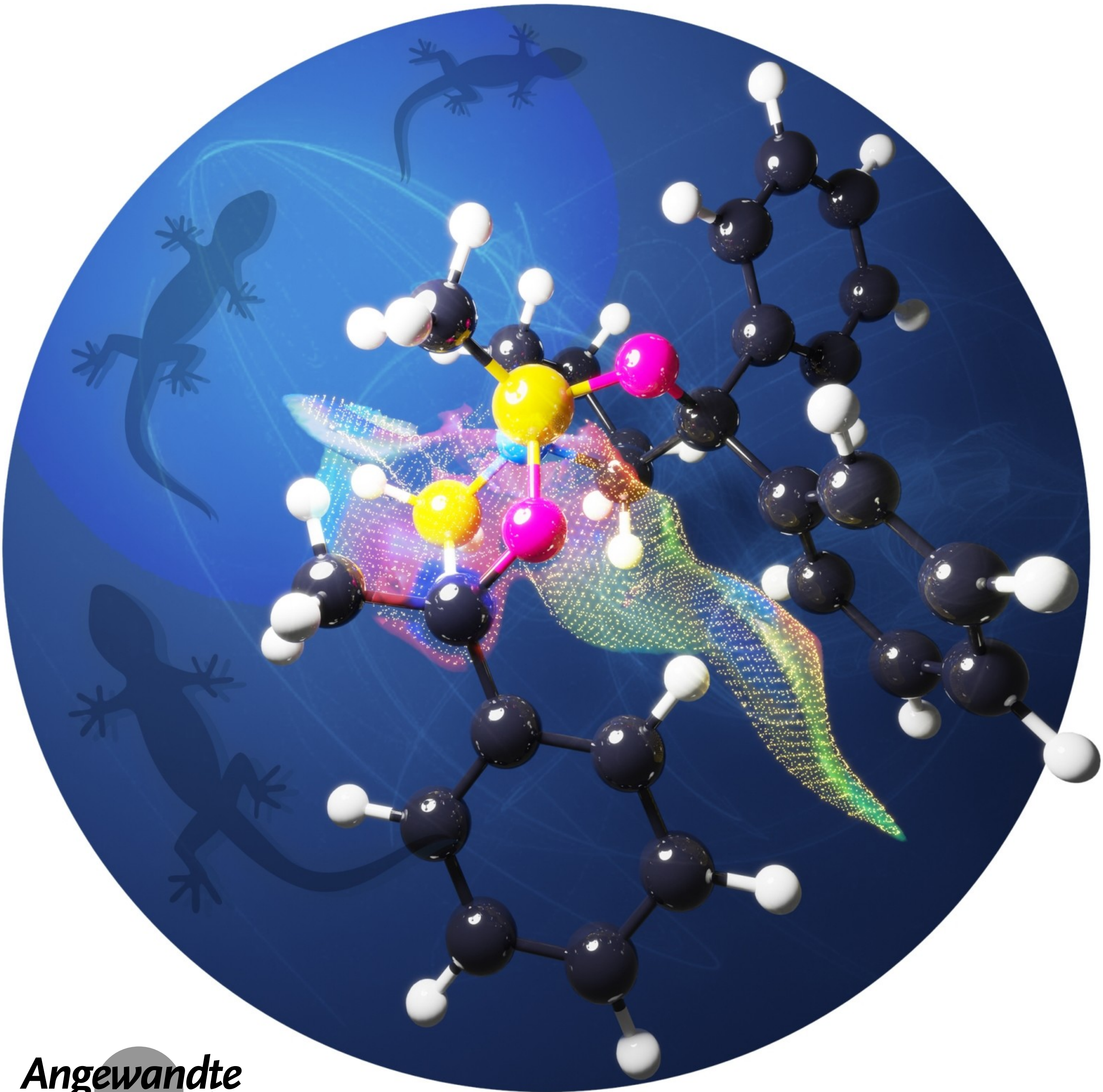

Abstract: London dispersion (LD) interactions are the main contribution of the attractive part of the van der Waals potential. Even though LD effects are the driving force for molecular aggregation and recognition, the role of these omnipresent interactions in structure and reactivity had been largely underappreciated over decades. However, in the recent years considerable efforts have been made to thoroughly study LD interactions and their potential as a chemical design element for structures and catalysis. This was made possible through a fruitful interplay of theory and experiment. This review highlights recent results and advances in utilizing LD interactions as a structural motif to understand and utilize intra- and intermolecularly LD-stabilized systems. Additionally, we focus on the quantification of LD interactions and their fundamental role in chemical reactions.

1. Introduction

J. D. van der Waals' famous maxim *"Matter will always display attraction"*[1] essentially constitutes the basis of all chemical processes. The complexity of reaction mechanisms, catalytic cycles or structural motifs can all be reduced to the fact that matter always displays attraction. Hence, as a perpetual physical concept, van der Waals (vdW) interactions govern molecular structures and chemical reactions[1a,2] as they reach from the simplest case of two atoms attracting each other noncovalently (observable at a low enough temperature) to complex systems, e.g., the folding of peptides,[3] catalyst-substrate recognition,[4] or the orientation of molecules in crystal lattices.[5] One of the main contributors to the attractive part of vdW interactions stems from electron correlation effects referred to as London dispersion (LD) interactions.[6] While molecular recognition and aggregation to a large extend are based on LD,[7] the explicit consideration of LD interactions in molecular systems has only been broadly conceptualized, quantified, and understood much more rigorously in the last decade.[7b]

LD interactions are described as quantum-mechanical fluctuations of the electron density leading to induced-dipole–induced-dipole interactions.[6b,8] Interestingly, London originally utilized spectroscopic properties to demonstrate the distance r^{-6} dependence of the attractive part of the vdW potential (1).[6d,9] As a result, he formulated the following mathematical equation, where C_6 represents an empirical polarization coefficient and r the distance between two atoms.

$$E_{disp} = -\frac{1}{2}\sum\frac{C_6}{r^6} \tag{1}$$

Although initially postulated by London in 1930 as the sum of pairwise interactions, σ–σ attraction has been mostly ignored for systems of larger size.[6c,d] This is not surprising considering the strength of a single pairwise interaction in comparison to point-charges. Consequently, LD interactions are considered to be significantly weaker than Coulomb interactions and mostly outweighed by Pauli (exclusion) repulsion as well. However, the dimerization of two atoms in the gas phase describes only the simplest case and can be extended by utilizing bulky moieties with multiple contacts, thereby rapidly increasing the number of pairwise LD interactions relative to other noncovalent interactions. The additivity of LD interactions helps rationalize various chemical as well as physical effects, i.e., the increasing boiling points or the differences in isomerization energies of linear and branched alkanes.[10] The concept of utilizing bulky and highly polarizable groups in order to increase LD interactions has evoked the term "dispersion energy donor" (DED) for such groups, in analogy to electron-donor substituents;[7b,11] of course, DEDs equally are dispersion energy acceptors via mutual polarization. LD interactions and the incorporation of DEDs intramolecularly stabilize labile structures, leading to their isolation. Examples include hexaphenylethane derivatives,[12] tetra-*t*butyltetrahedrane,[13] tetrakis(trimethylsilyl)tetrahedrane (Figure 1, left),[14] and structures containing a Sn–Sn double bond.[15] (Figure 1, middle). All structures benefit from a "protective LD shell"

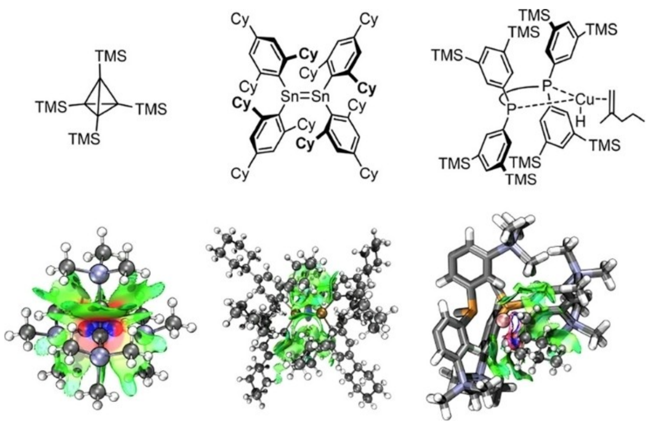

Figure 1. Intramolecular NCI plots of tetrakis(trimethylsilyl)tetrahedrane[14] (left), $[Sn(C_6H_2\text{-}2,4,6\text{-}Cy_3)_2]_2$ (Cy = cyclohexyl, middle),[15] and the favored *si* face hydrocupration transition structure according to Hartwig et al.[17] (selected functional groups omitted for clarity). Isosurfaces (isovalue *s* of 0.5, ranging from $\text{sign}(\lambda_2)\rho = -0.05$ to $+0.05$ a.u.) are color-coded red (indicating strong repulsion), blue (strong attractive interactions), and green (corresponding to weak NCIs). Reprinted with permission from Schreiner et al.[18] Copyright (2022) American Chemical Society.

[*] Dr. L. Rummel, Prof. Dr. P. R. Schreiner
Institute of Organic Chemistry, Justus Liebig University
Heinrich-Buff-Ring 17, 35392 Giessen (Germany)
E-mail: prs@uni-giessen.de

around a fragile core resulting in thermodynamic as well as kinetic stability. To quantify and qualify the effects of DEDs on structure, molecular balances were designed.[16]

In recent years the importance of LD interactions as a chemical design element has been assessed in a variety of research areas. Emphasis was placed on quantifying the interactions between various DEDs to utilize LD as a source of thermodynamic stability or driving force.

As a consequence, new computational and experimental approaches had to be developed to measure and separate LD from other (noncovalent) interactions. In this process many new structures were designed to determine the balance between attractive and repulsive interactions. Here, the focus was not only on the well-established π-π and σ-π interactions, but much more so on σ-σ attraction. To quantify such interactions many novel intra- and intermolecular dispersion-stabilized structures were prepared.

While the presence of LD interactions can be readily demonstrated both computationally and experimentally in the gas phase, the compensation of LD due to solvation was discussed extensively in recent years.[19] Multiple systems were developed to investigate the interactions of bulky groups in various solvents or through direct comparison between gas phase and solvent measurements.

The most sizable effect of LD interactions is apparent through the control of reactivity due to incorporation of DEDs.[7b,11] Especially in the area of catalysis, the role of LD interactions proved to be of key importance in molecular recognition, substrate activation, transition state lowering, and as chemical driving force (Figure 1, right).

As a result, LD interactions have now become a veritable tool to synthesize novel structures, increase selectivities, or facilitate alternative reaction pathways. At the same time, LD interactions have been introduced into chemical education to improve students′ understanding of such structure–property relationships.[20] Oddly, they have—at the stage of writing this review—not yet found entry into chemistry textbooks.

This review intends to highlight the main advances in understanding, sizing, and controlling LD interactions. As the topic was reviewed here in 2015,[7b] we mostly focus on the developments of the last eight years. During this time a priority program on LD (SPP 1807 "Dispersion") of the Deutsche Forschungsgemeinschaft (German Research Council) was established to investigate the effects of LD on structure and reactivity in molecular chemistry.

1.1. Structure of the Review

We first discuss several areas that highlight the importance of LD interactions and will then discuss the broader implications. For a general introduction to LD interactions, we refer the reader to our review article of 2015.[7b]

A thorough examination of LD interactions can only be achieved through a tight interplay between theory, spectroscopy, and synthesis. Therefore, we begin with methods to elucidate LD and noncovalent interactions in general. Theoretical considerations and experimental approaches to quantify LD interactions have been extended and refined in

Lars Rummel studied chemistry and biology at the Justus Liebig University Giessen, Germany, to become a teacher. In parallel, he received his B.Sc. degree in chemistry in 2018. He joined the group of Peter R. Schreiner as research associate in 2019 and completed his doctoral degree in 2023. His research focuses on the effects of London dispersion interactions on molecular structure and reactivity. In the years 2021 and 2022, he served as the scientific secretary of the priority program on dispersion (SPP 1807) of the Deutsche Forschungsgemeinschaft (German Research Council).

Peter R. Schreiner studied chemistry in his native city at the University of Erlangen-Nuremberg, Germany, where he received his Dr. rer. nat. (1994) in Organic Chemistry. Simultaneously, he obtained a PhD (1995) in Computational Chemistry from the University of Georgia, USA. He completed his habilitation at the University of Göttingen (1999), before becoming associate professor at the University of Georgia, and head of the institute in Giessen in 2002. P. R. Schreiner is an elected member of the Leopoldina—German National Academy of Sciences, the North Rhine-Westphalian Academy of Sciences, Humanities, and the Arts, the Academy of Science and Literature (Mainz), the Berlin-Brandenburg Academy of Sciences, and is a Fellow of the Royal Society of Chemistry. He received the Dirac Medal (2003, WATOC), the Adolf-von-Baeyer Memorial Award of the GDCh in 2017, the RSC Award in Physical Organic Chemistry in 2019, the Academy Award of the Berlin-Brandenburg Academy of Science in 2020, and the ACS Arthur C. Cope Scholar Award 2021. He is the 2024 recipient of the Gottfried-Wilhelm-Leibniz Award of the Deutsche Forschungsgemeinschaft (DFG). He has been a visiting professor at the CNRS in Bordeaux, the Technion in Haifa, the Australian National University in Canberra, and the University of Florida in Gainesville. His research interests include organic reaction dynamics and reactive intermediates, quantum mechanical tunneling as well as London dispersion interactions as probed in the realm of nanodiamonds and organocatalysis.

recent years. In the first section, we provide an overview of newly developed approaches to single out LD interactions.

The second section focuses on implications of LD on molecular structures. By demonstrating exceptional structural motifs only accessible through LD, we shift our focus to the spectroscopic prospects and advancements made by studying small energy differences.

Thirdly, we consider reactivity and highlight the role of LD interactions. We close in demonstrating the influence of LD on stereoselective catalysis.

2. Elucidation of London Dispersion Interactions

The knowledge of the ubiquitously present attraction that atoms and molecules have, has been around for over 150 years.[1a,6b,c,8a] Nevertheless, the methods to quantify LD interactions and to differentiate them from other effects have been developed much more recently. In the first part of this section, we discuss the current computational methods to analyze and describe LD interactions, while the second part concentrates on their experimental evidence. By highlighting the advantages and disadvantages of molecular balances, we also outline ways to assess LD interactions in solution.

2.1. Theory and Computations

In recent years, computational chemistry has made important progress in identifying and quantifying LD interactions. We consider advances made in density functional theory (DFT) and wave function theory (WFT). On the DFT side, Truhlar et al. had made significant progress in including improved descriptions of medium-range electron correlation in elaborately parametrized functionals to capture noncovalent interactions; these approaches have led to the very broadly used “Minnesota Functionals”.[21] The most recent approaches of this group to capture LD are flexible, single hybrid functionals that depend on the density and the occupied orbitals on the one hand and on a damped LD term that varies with geometry on the other.[22]

Another approach comes from the Corminboeuf group who introduced a density-dependent correction (dDsC) to DFT that builds on the reformulation of the exchange hole dipole moment, thereby improving the interaction energy, in particular, for the intramolecular case.[23] The dDsC approach aims at balancing long-range correlation and the DFT-inherent delocalization error.

An entirely different strategy was introduced by Tkatchenko and Scheffler who developed a parameter-free method for the accurate determination of long-range interactions from mean-field electronic structure computations. The interatomic C_6 coefficients where thus derived from the electron density and highly accurate reference data for the free atoms.[24]

One of the most common and popular approaches to account for LD interactions is to utilize an empirical dispersion correction (often denoted as DFT-Dn, with $n=1$–4).[11,25] Grimme and co-workers have developed these approaches over the last decade. A force-field-type term is added *a posteriori* to a DFT energy.[26] The amount of LD in a system can be estimated using simple isodesmic equations and by comparison of the energies computed with or without inclusion of a DFT-Dn correction.[13b] This *ad hoc* correction is one of the most popular approaches of dealing with LD interactions since its computational cost is quite reasonable.[26] Whereas other methods[21a,27] utilize the electron density to take local dispersion coefficients into account, Grimme's DFT-Dn corrections only use the atomic positions to generate the dispersion coefficients with respect to the neighboring atoms from reference values.[28] Additionally, damping functions are employed at close interatomic distances to deal with high variations of dispersion forces.[29] The most recently published D4 correction is an improvement over the DFT-D3 correction, which did not handle charged systems well.[30] D4 is still solely based on geometries and atomic positions but includes a scaling of the dispersion coefficients based on atomic charges and electronegativity (Figure 2). Although D4 generally outperforms D3, the differences are most apparent for transition metal complexes.[31]

The analysis and quantification of LD interactions is not only important for DFT computations but also in WFT. With this in mind, Neese et al.[32] reported in 2016 a novel way to decompose interaction energies of the domain-based local pair natural orbital coupled-cluster (DLPNO-CCSD(T)) method[33] into physically interpretable components. The method, called Local Energy Decomposition (LED),[32] differentiates between electrostatic, electronic promotion, exchange, dynamic charge polarization, and LD interactions ranging from weakly to strongly bound dimers. It can be applied to an optional number of fragments giving accurate results at the coupled cluster level. Using the counterpoise correction of Boys and Bernardi,[34] the method intrinsically accounts for the basis set superposition error (BSSE). Within this supramolecular approach the bond dissociation energy (ΔE_{BDE}) is initially decomposed into an electronic interaction term (ΔE_{int}) and a geometric preparation energy ($\Delta E_{\text{geo-prep}}$), which accounts for the

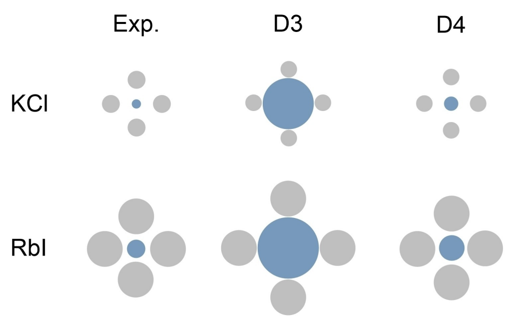

Figure 2. Schematic representation of anionic (grey) and cationic (blue) polarizability values of KCl (top) and RbI (bottom) in a comparison between experimental results (left), computed D3 (center) and D4 (right) atomic polarizabilities. Adapted from Grimme et al.[31b]

energy necessary to deform the monomers into the dimer structure (2).

$$\Delta E_{\mathrm{BDE}} = \Delta E_{\mathrm{int}} + \Delta E_{\mathrm{geo\text{-}prep}} \tag{2}$$

The interaction energy is further split into a Hartree-Fock and a correlation contribution. By decomposing both Hartree-Fock and correlation energy, Neese et al. developed a nonperturbative approach to compute intermolecular interactions. The method allows dissecting a variety of noncovalent interactions ranging from dispersively bound dimers to ionic interactions into chemically useful energies. As shown below, such an energy decomposition analysis (EDA)[35] results in a detailed characterization of the dissociation energy whereas electronic preparation (intra-fragment contribution $\Delta E^{\mathrm{HF}}{}_{\mathrm{el\text{-}prep}}$), electrostatic ($E_{\mathrm{elst}}$), and exchange ($E_{\mathrm{exch}}$) interactions result from decomposition of the HF term. The correlation energy can be separated into charge-transfer (E_{ct}), dispersion (E_{disp}), and electronic preparation ($\Delta E^{\mathrm{C}}{}_{\mathrm{el\text{-}prep}}$) contributions as well (3).[32]

$$\begin{aligned}\Delta E_{\mathrm{BDE}} &= \Delta E^{\mathrm{HF}}{}_{\mathrm{el\text{-}prep}} + E_{\mathrm{elst}} + E_{\mathrm{exch}} + \Delta E^{\mathrm{C}}{}_{\mathrm{el\text{-}prep}} \\ &+ E_{\mathrm{ct}} + E_{\mathrm{disp}} + \Delta E_{\mathrm{geo\text{-}prep}}\end{aligned} \tag{3}$$

The main advantage over symmetry adapted perturbation theory[36] (SAPT) is that LED allows to dissect strong and weak interactions at the same level of theory whereas SAPT only examines weak interactions via its perturbative approach. Interestingly, the intermolecular exchange term differs from the exchange contribution in SAPT.[32] Whereas the exchange term represents a repulsive interaction in SAPT, it is a stabilizing term within LED. Nevertheless, a comparison of SAPT and LED has shown that both energy decompositions to be in overall good agreement for the distance-dependence of noncovalent interactions.[37] The LED method was utilized by Neese et al.[38] for investigations of LD effects in frustrated Lewis pairs (FLPs). Accordingly, increasing DED size increases thermodynamic FLP stability. Additionally, Bistoni and co-workers showed that LD significantly contributes to the stability of metal complexes through coordination to C–H σ-bonds. They studied agostic complexes[39] where around 50 % of attraction is due to LD, and a variety of direct σ-complexes,[40] in which the LD energy amounts to at least 67 % of the overall binding energy. Other noncovalent interactions, e.g., H-bonding, can be studied with the LED method as well.[32] Furthermore, it can also be applied to open-shell systems by computing energies at the UHF-DLPNO-CCSD(T) level of theory.[41]

A subsequent non-empirical method applicable to very large systems is the newly developed Hartree-Fock plus London dispersion (HFLD) scheme.[42] In HFLD, the interaction energies are computed at the HF level of theory and corrected with an LD term computed at CCSD. Since all other intramolecular correlation energies compensate each other and can therefore be neglected, the method efficiently quantifies intermolecular interactions.

Since SAPT[43] is still the most popular energy decomposition analysis to date, we will briefly present its main features. As mentioned before, SAPT allows computing the interaction energy of two molecular fragments using a perturbation of the Hamiltonian of both fragments.[36] Thus, the energy is partitioned into electrostatics (E_{elst}), exchange (E_{exch}), induction (E_{in}), and dispersion (E_{disp}) according to equation (4):

$$\Delta E_{\mathrm{int}} = E_{\mathrm{elst}} + E_{\mathrm{exch}} + E_{\mathrm{in}} + E_{\mathrm{disp}} \tag{4}$$

Here, the electrostatics describe the interaction of charge densities of multipoles and hence is attractive. Different from LED, the exchange term describes repulsive interactions caused by an overlap of wavefunctions (Pauli repulsion). Due to different definitions, this term cannot be compared to the LED exchange term. In a second-order expansion, SAPT generates energies for LD and induction, i.e., the redistribution of an electric charge due to the electric field of the opposing monomer.[36] Since SAPT and LED are based on different theories, only electrostatics and dispersion energies can be readily compared. Additionally, due to the perturbative approach only weak interactions can be described properly with SAPT.[32] Improvements of the SAPT scheme focus on adjusting the second-order induction and dispersion energies. By employing the GW approximation (an approach based on the Green′s function G and the dynamically screened Coulomb interaction W) and response functions from Bethe-Salpeter equation (BSE),[44] Klopper and co-workers achieved more accurate results as compared to DFT-SAPT.[45] In order to address the slow basis set convergence in conventional perturbational dispersion approaches, Patkowski et al.[46] utilized a method from explicitly correlated (F12) electronic structure theory. The method was utilized to investigate complexes involving heavy elements such as gold, mercury, and bismuth.[47] Utilizing SAPT, Herbert et al.[48] revisited the dimerization of benzene and larger polycyclic hydrocarbons. While benzene dimers are commonly described as a result of quadrupolar electrostatic interactions, the C_6H_6–C_6F_6 dimer already contradicts the model based on quadrupolar effects as it also favors the periplanar offset dimer.[48c] Alternatively, a competition between LD and Pauli repulsion dictates π-π interactions resulting in the offset stacked benzene dimer. In stark contrast to textbook knowledge, electrostatic interactions are not the origin of this geometric preference (Figure 3).[49]

Visualizing LD greatly helps understand the effects of DEDs between interacting moieties. Popular are noncovalent interaction (NCI),[50] Dispersion Interaction Density (DID) plots,[51] and London Dispersion Potential (LDP) maps.[52] The NCI approach is based on a 2D plot of the reduced density gradient and the electron density. By depicting isosurfaces of the reduced density gradient together with electron densities, the strength of noncovalent bonding can be estimated. High densities represent strong interactions, whereas lower densities hint to weaker interactions. By accounting for the sign of the electron density values, attractive and repulsive interactions can be separated

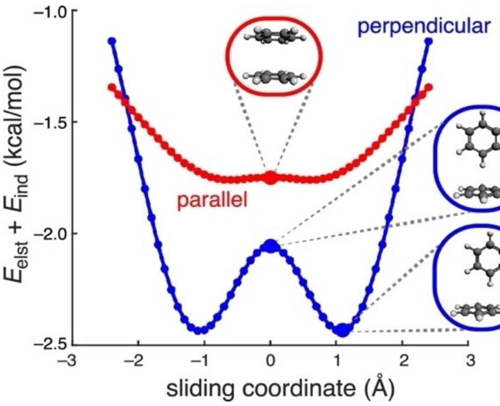

Figure 3. Polarized electrostatic and inductive interactions along a sliding coordinate with benzene oriented either parallel (red) or perpendicular (blue). Note that $E_{elst} + E_{ind}$ fail to reproduce the geometric preference of the benzene dimer. Reprinted with permission from Herbert.[49] Copyright (2021) American Chemical Society.

and visualized according to a color-code. Strongly repulsive interactions via Pauli repulsion are depicted in red, while strongly attractive forces are coded blue. Green isosurfaces represent weak interactions like dispersion or dipole interactions.[50] In order to properly distinguish between the types of weak interaction, dispersion interaction density (DID)[51] plots can be utilized, visualizing LD interactions to locate the origin of stabilization. These plots are usually depicted as a voxel or wireframe plot through coloring of the local intermolecular interaction density. Here, the color scheme ranges from red (strong LD interaction) over green to blue (no dispersion interaction). Additionally, Pollice and Chen introduced London dispersion potential (LDP) maps as quantitative LD descriptors.[52] By using a parameter P based on homoatomic dispersion coefficients, the authors defined P_{int}, which not only accounts for the spatial polarization distribution but also for the ionization potentials in molecules with respect to their vdW surface.[52–53] This parameter was then applied to the periodic table and DEDs to highlight the coherence of dispersion coefficients and atomic radii. By projecting the P values onto the electron density isosurface, a three-dimensional depiction quantifies and visualizes LD interactions within molecules. The color scheme was chosen to coincide with DID plots. In comparison to the other depictions, LDP portrays the dimer LD contact areas, while DID plots highlight the origin of these interactions. Figure 4 displays a comparison of all visualization tools according to Pollice and Chen.[52]

It is fair to say at this stage that there is a variety of computational tools and techniques to identify and quantify LD interactions in molecular systems. The application of these tools is straightforward and computationally inexpensive.

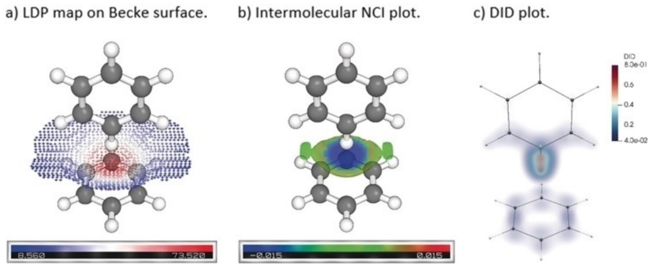

Figure 4. NCI visualization methods in the T-shaped benzene dimer. a) LDP mapped onto the intermolecular Becke surface (values in $kcal^{0.5}\,mol^{-0.5}$). b) Intermolecular NCI plot (values in au). c) DID plot (values in $kJ\,mol^{-1}\,Bohr^{-3}$). Reprinted with permission from Pollice and Chen.[52] Copyright (2019) John Wiley and Sons.

2.2. Experimental Manifestations of London Dispersion Interactions

Molecular balances have been the workhorse to analyze LD interactions experimentally.[19a,54] Hereby, interactions between various hydrocarbon moieties are in focus, and the acquired knowledge can readily be transferred to other molecular systems.

Molecular balances typically measure the thermodynamic energy differences of conformers or configurational isomers, and the equilibrium constants are indicative of noncovalent interactions that affect the isomers to different degrees (Figure 5). An obvious criterion worth mentioning is that the geometric change must be readily quantifiable by means of spectroscopic techniques. Additionally, intramolecular interactions have to be definable and separable. Just as well, ionic interactions[55] or hydrogen bonding,[56] which might exceed LD interactions in magnitude for intermolecular contacts must be considered. Thus, systems including heteroatoms have to be treated with caution. Solvent effects have to be taken into account also.[19e,57] Especially in highly polar solvents solvophobic effects were reported, which minimize balance-solvent interactions while maximizing solvent-solvent interactions.[58]

The most well-known molecular balance was reported by Wilcox and co-workers in 1994.[16] The rigid scaffold, based on Tröger's base, limits the number of thermodynamically accessible conformers to two torsional isomers that

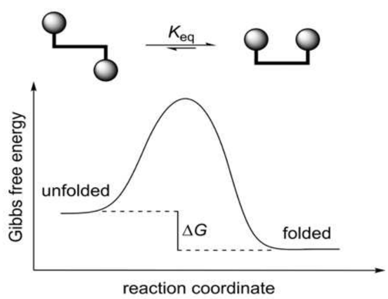

Figure 5. Schematic illustration of a molecular balance consisting of a folded and an unfolded conformer (or configuration).

interconvert at room temperature. Based on NMR analysis, Wilcox and co-workers determined the ratio of folded to unfolded isomers, whereby noncovalent edge-to-face aromatic interactions in the folded conformer were assigned to having a stabilizing effect. On the other hand, entropy drives the equilibrium towards the unfolded isomer. The expected CH-π interactions between the aromatic groups could be observed by NMR and X-ray crystallography and stabilize the folded conformer by $\Delta G_{\text{fold}} = -0.24\ \text{kcal mol}^{-1}$. Additional substitution in *para* position of the aromatic ester favors the T-shaped noncovalent contact even further. By substituting the aromatic ester with a cyclohexyl or *tert*-butyl ester, Wilcox and co-workers noticed that the resulting σ-π interactions were as dominant as the edge-to-face aryl-aryl interactions. This suggests large LD interactions between the aryl and the alkyl groups rather than electrostatic attraction.[59] Additionally, Wilcox also noticed a slight variation in the hinge angle of the backbone of the torsion balance, thereby maximizing the attractive interactions.[16]

By focusing on alkyl-alkyl interactions, Cockroft and co-workers substituted Wilcox' balance with long alkyl chains (R = *n*-heptyl; R′ = *n*-hexyl) in the aromatic *para*-positions of the balance (Figure 6).[57] Measuring the equilibria in various polar, apolar, and fluorous solvents, they came to the conclusion that solvophobic effects largely cancel LD interactions, as corroborated by dissecting the interaction energy of the alkyl substituents using a double mutant cycle. This, however, contradicts Wilcox' original findings, namely that no significant solvent effects were observed.[16,57] Subsequent studies by the Cockroft group using perfluoroalkyl chains (R=R′ = perfluoro-*n*-hexyl) as substituents demonstrated the competition of intramolecular and intermolecular LD.[60] By correlating Gibbs free energies of alkyl or perfluoroalkyl substituents with the cohesive energy densities of the solvents, a linear regression analysis demonstrated that both LD interactions and solvophobic effects are responsible for the folding of the Wilcox balance. While the former is dominant in apolar organic and fluorous solvents, the latter is most prominent in aqueous and highly polar solvents.[60a,61]

In order to study aromatic stacking interactions, Shimizu and co-workers designed a molecular balance based on a bicyclic *N*-arylimide scaffold. In comparison to Wilcox' balance, which was used to quantify edge-to-face aromatic interactions, Shimizu and co-workers set up a framework with a distance of 3.75 Å between arene groups to measure face-to-face interactions.[62] After studying substituent effects,[63] Shimizu et al. focused on quantifying LD interactions influencing the stacking behavior of arene groups.[64] By accounting for conflicting effects (e.g., solvophobic or linker effects) using the corresponding control balances and double mutant cycles, Shimizu and co-workers quantified the LD interactions required for molecular folding. Conflicting with computational studies,[65] they came to the result that LD interactions only play a minor role in the stacking behavior of aromatics. Furthermore, they suggested LD compensation due to solvent effects.

Later, Shimizu et al. demonstrated the importance of LD while studying σ-π interactions (Figure 7).[66] Depending on the attached group and the substitution pattern, either attractive or repulsive interactions dominate. By exchanging one side of their balance with *meta* or *para* substituted benzenes, the distance dependence of LD and Pauli repulsion was highlighted. As a result, they concluded an optimal distance for σ-π interactions of 2.5 to 3.0 Å.

Other than conformational balances, Chen et al. developed a method to quantify LD interactions using dissociation energies of weakly bound dimers.[19d] They used protonated *N*-heterocyclic compounds that can dimerize via hydrogen bonding (Figure 8). In addition to this central connection, every monomer possesses remote substituents interacting intermolecularly via LD. As a result, LD

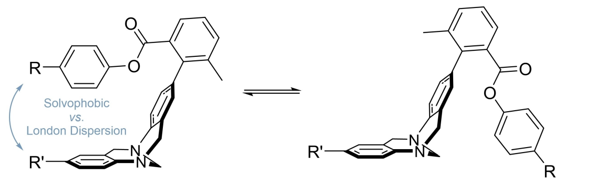

Figure 6. Molecular balance utilized by Cockroft and co-workers to partition solvophobic and LD interactions in various solvents.[60a]

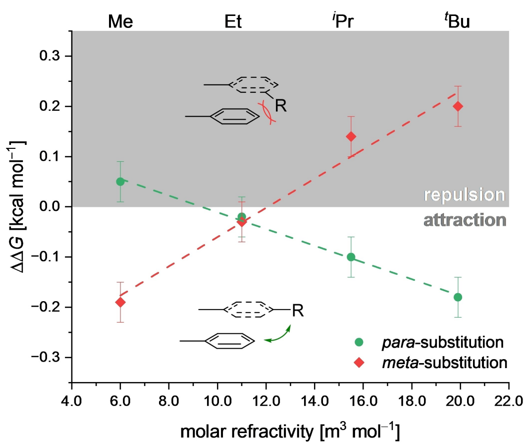

Figure 7. Differential interaction free energies $\Delta\Delta G$ derived from a double-mutant cycle for alkyl-π interactions. While *meta* substitution (red markings) shows repulsive interactions, the *para* substitution pattern (green markings) highlights attractive LD. Adapted from Shimizu et al.[66]

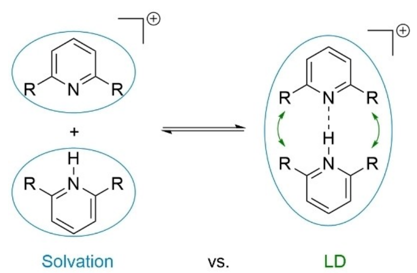

Figure 8. LD supported formation of proton-bound dimers and compensating solvation effects. Adapted from Chen et al.[19d]

interactions are predominantly at work in the proton-bound dimer. The dissociation energies were thoroughly studied using a large set of protonated *N*-heterocyclic compounds ranging from amines to pyridines and quinolones. The dimerization process was investigated computationally and experimentally, both in the gas phase and in solution. As a result, Chen et al.[19d,53] found considerable influence of LD interactions in the gas phase. By performing threshold collision-induced-dissociation measurements (T-CID), they could directly compare computational and experimental data. In order to account for solvent effects, free bond dissociation energies were measured in dichloromethane via variable temperature NMR experiments. As a result, a compensation of around 70 % of intermolecular LD was reported due to additional solvent-solute interactions.[19d] Interestingly, these effects could not be reproduced exactly by the computations using state-of-the-art solvent models. Implicit solvent models, e.g., SMD[67] and COSMO-RS,[68] should therefore perhaps be treated with caution when trying to account for LD interactions.

In 2017, Albrecht and co-workers investigated the effect of LD on the dimerization processes of metal complexes (Figure 9).[58] Using helicate-type titanium(IV) triscatecholate complexes, they measured the equilibrium constant of the dimerization in the presence of lithium ions. The catechols were systematically substituted by altering the ester moiety. The effects of linear, branched, *n*-fluorinated, and cyclic substituents were considered. Enthalpy and entropy contributions were determined via van't Hoff analysis in addition to the equilibrium constants. By elongating the alkyl chains, the dimerization process becomes enthalpically more favorable. On the other hand, entropy disfavors the dimeric structure due to restrictions of torsional motions. The equilibrium shifts to monomeric titanium complexes with branched alkyl attachments, suggesting an increase in repulsion in the dimer. The entropic penalty of close alkyl-alkyl contacts slightly decreases in cyclic compounds, making the dimer the energetically preferred structure. The trend of fluorinated *n*-alkyl chains was comparable to hydrogenated chains but significantly smaller. By comparing the equilibrium constants of the *iso*-propyl and cyclobutyl system, Albrecht et al.[58] noticed a substantial difference although both groups are comparable in size. The difference is caused by larger enthalpic contributions of the rigid cyclic derivative due to attractive LD rather than the bulkiness of the molecules under consideration. Accordingly, they deduced that solvophobicity of the alkyl groups plays a minor role in their system. In a second study, the cyclohexyl substituted system was investigated with respect to the conformational axial/equatiorial preference in the dimeric structure.[69] Counterintuitively, the axial orientation is favored due to a combination of LD and solvophobic effects, while the equatorial position does not offer stabilizing noncovalent interactions between neighboring groups.

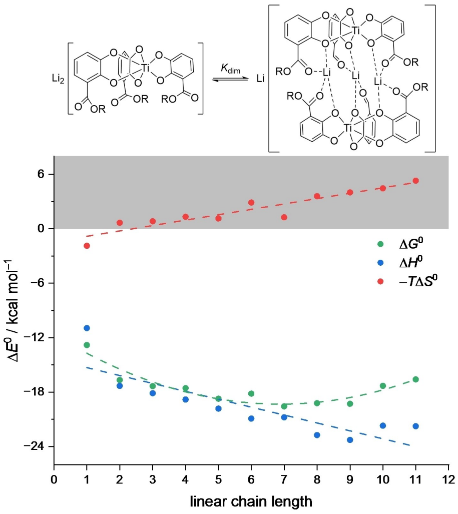

Figure 9. Energy contributions of titanium complexes with increasingly long linear alkyl substituents. Enthalpy (blue markings) and entropy (red markings) are experimentally determined via van't Hoff analysis. Gibbs free energies (green markings) indicate stabilizing effects with increasing chain length. Adapted from Albrecht et al.[58]

A purely hydrocarbon based molecular balance can be designed using cyclooctatraene (COT), initially presented by Streitwieser et al.[70] in 1981. Since it avoids heteroatoms, it minimizes alternative noncovalent binding interactions, e.g., hydrogen bonding or electrostatic interactions. Streitwieser et al.[70] noticed the unusual equilibrium position of 1,6- vs. 1,4-di-*tert*-butyl-COT, which was later experimentally confirmed by Hanzawa et al.;[71] the results are also supported by computations.[72] Even though COT is non-planar, it undergoes a valence-bond isomerization that exchanges the 1,4- with the 1,6-substituent positions. While the 1,4-isomer places the *tert*-butyl groups far away from each other, the 1,6-isomer brings them in close proximity. As recognized already by Streitwieser et al.[70,73] this close contact is stabilizing, even in solution as evident from the determination of the equilibrium constant via NMR in $CDCl_3$. In 1992, Anderson and Kirsch reported on additional substitution patterns, demonstrating the LD distance-dependence.[74] By varying the sizes of the attached groups and investigating the equilibrium via NMR analysis, they observed a preference for the 1,6-isomer. With increasing substituent size from methyl to *tert*-butyl, the ensuing enthalpic stabilization increasingly favors the 1,6-isomer. In 2021, Schreiner et al.[19e] re-investigated the 1,4-/1,6-COT balance to determine the solvent effects on the equilibrium. Measuring equilibrium constants in 16 different organic solvents via variable-temperature NMR experiments shows an excellent correlation of LD with solvent polarizability. Irrespective of the solvent, the more crowded 1,6-isomer dominates at r.t., whereas only at high temperatures the equilibrium slightly favors the entropically favored 1,4-isomer. Hence, LD persists in any measured solvent even though the enthalpic and entropic contributions vary. Their change in opposite directions results in very similar free energies for any solvent tested.

The COT backbone was further exploited to study the effects of silyl groups with respect to their steric size[18,75] and role to act as DEDs (Figure 10).[11] Silyl groups are larger than alkyl groups and more polarizable so they are expected

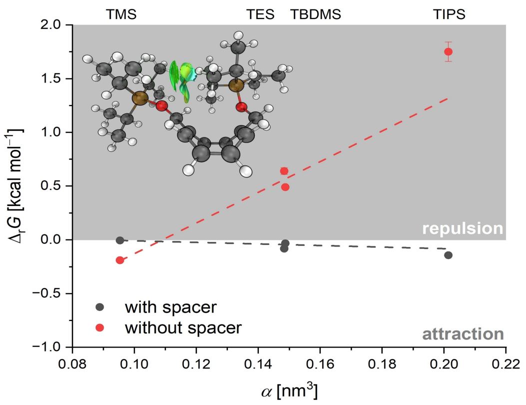

Figure 10. Gibbs free energies for the equilibrium of silyl substituted COT without (red markings) and with (grey markings) spacer group. The depicted molecule (TIPS substituted COT with spacer) highlights the role of LD via an NCI-plot. The green isosurface corresponds to LD.[18]

to be excellent DEDs. By directly attaching silyl groups at the COT molecular backbone, the relative bulkiness of such groups was investigated and successfully correlated to literature known steric parameters, such as A-values,[76] solvolysis rates,[77] and Tolman's steric parameter θ.[78] The main driving force favoring the unfolded isomer was found to be internal strain within the COT backbone. On the other hand, when a –CH_2O– spacer group is placed between COT and the silyl groups, NMR measurements reveal that the bulky TIPS group shifts the equilibrium between 1,4- and 1,6-disubstituted COT furthest towards the folded and more crowded valence isomer.[18] With a computationally derived internal strain for TIPS-COT of 1.2 kcal mol^{-1}, attractive LD is responsible for the remaining 0.7 kcal mol^{-1}. However, flexibility due to the –CH_2O– spacer comes at the cost of unfavorable folding entropy.

Finally, the COT molecular backbone was further exploited to experimentally study hydrogen bonding via a model system resembling the cyclic water dimer transition structure.[79] Remarkably, an energy decomposition analysis demonstrates that hydrogen bonding in this case is largely dominated by electrostatic and LD interactions. While the first constitutes around 65 % of the total hydrogen bonding interaction energy, the latter is responsible for around 25 % stabilization.

Another purely hydrocarbon-based molecular balance that undergoes a configurational isomerization of a double bond is comprised of a 9,9′-bifluorenylidene backbone substituted in the 2,2′-positions with various alkyl groups. This system can readily be equilibrated thermally or photochemically between *Z*- and *E*-configurations.[80] Originally, Minabe et al.[81] synthesized 2,2′-diacyl balances as fullerene precursors and noticed an unexpected *Z*/*E* ratio after connecting two fluorene moieties in the 9,9′-positions. While the 2,2′-diacetyl derivatives gave a *Z*/*E* ratio of 30/70, the 2,2′-distearoyl balance afforded a 90/10 ratio in favor of the sterically more demanding *Z* conformer; this demonstrated the "sticky" properties of fatty acids. Minabe and coworkers already suggested in 2000 LD as the key factor for selectivity.[81] In 2022, Schreiner et al.[80] reinvestigated the system removing the acyl functional groups to isolate and quantify the LD interactions. By systematically exchanging alkyl groups in 2,2′-position with increasing polarizability the interplay of repulsive and attractive interactions as well as solvent effects were studied via NMR spectroscopy. While linear alkyl chains favor the folded *Z*-isomer despite an entropic penalty, the experimental ratios of bulky substituents, e.g., *tert*-butyl and cyclohexyl substituents, do not systematically increase with substituent size (Figure 11). A computational analysis revealed a more complex interplay of LD, steric hindrance, and solvent accessibility, and ultimately resulted in identifying cyclohexyl ($\Delta G = -0.60$ kcal mol^{-1} in cyclohexane) as the strongest DED. Whereas methyl substitution results in a 1:1 mixture of *Z*- and *E*-isomers, ethyl as well as *iso*-propyl groups shift the equilibrium towards the more crowded *Z*-isomer (Figure 11). The fine line between attraction and repulsion is best observed by comparing cyclohexyl to *tert*-butyl substitution. While cyclohexyl favors the *Z*-form by maximizing LD due to perfect alignment of both cyclohexyl substituents, the more rigid *tert*-butyl substituent on the other hand reverses the effect due to increasing repulsive interactions. Whereas some studies[19d,57] suggest a decrease of LD in solution, the 9,9′-bifluorenylidene molecular balance gave similar experimental results for all solvents employed (cyclohexane, toluene, benzene, bromobenzene, pyridine, nitrobenzene, and acetic acid).

2.3. London Dispersion in Solution

As partially addressed above, in all molecular balances some compensation of LD can be observed when comparing

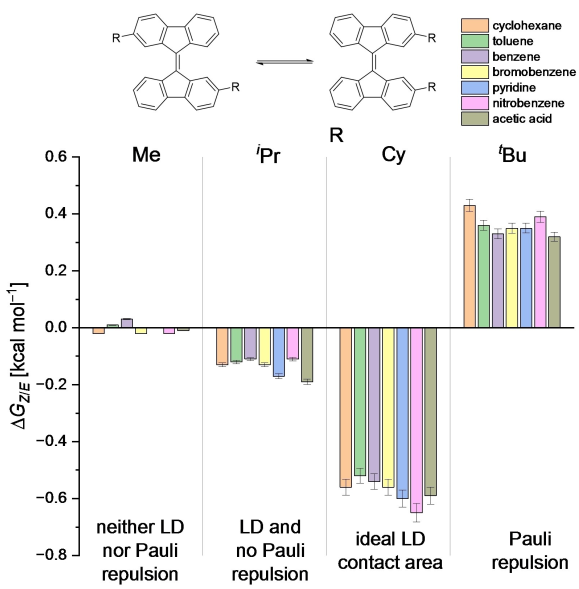

Figure 11. Gibbs free energies for the equilibrium between *Z*- and *E*-isomers of 9,9′-bifluorenylidene molecular balances at 333 K in various solvents.[80a]

computations or gas phase interaction energies with those in solution. While the importance of solvation is undisputable, the effects of LD in solution are still present and noticeable.

In general, two reasons can be identified as counteracting forces opposing the dimerization process of two molecules as well as two molecular fragments of a molecular balance. The first factor compensating attractive interactions is entropy, which is usually negative for a dimerization.[54b,c,58] Additionally, by increasing the monomer size the enthalpic gain due to LD is always compensated by an increasing entropic penalty due to restrictions in rotational and vibrational degrees of freedom. The number of atoms present in a dimerization process does not only rapidly increase the number of pairwise interactions but also the degrees of freedom in the monomers. For flexible molecules the tight interplay of solvation and entropy must be taken into account when evaluating Gibbs free energies.[18,82] In every balance discussed above this entropic penalty counteracts LD.[54b,c,58] By weighing LD against cation-π interactions utilizing large flexible pyridinium cations Chen and co-workers highlighted the challenges to *in silico* predict the complex interplay of LD and entropic compensation.[83] While computations predicted LD to be dominant, gas-phase cryogenic ion vibrational predissociation (CIVP) spectroscopy found the effects of *tert*-butyl groups to be modest.

While computational investigations suggest LD to play a dominant role for molecular aggregation in the gas phase, its effects in solution are still discussed extensively.[19,84] Although stabilizing LD effects were demonstrated with various molecular balances and even catalytic processes, studies suggest partial compensation of LD by solute-solvent interactions. Interestingly, both phenomena (solute-solute as well as solute-solvent interactions) largely originate from LD interactions.[19c,54b,c] Instead of intramolecular stabilization, the energy gain via intermolecular solute-solvent contacts can hamper molecular dimerization and aggregation.

By computationally studying Wilcox' torsional balance Nakamura and Houk initially described an equilibrium between intramolecular van der Waals contacts and intermolecular solute-solvent interactions.[85] An overestimation of 1–3 $\mathrm{kcal\,mol^{-1}}$ of the preferred folded conformer in the gas phase could only be explained by taking solvation effects into account. Thereby, a compensation of the relative instability of the unfolded balance was achieved by including interactions between solvent molecules and the molecular balance itself. The same balance was subjected to experiment to dissect the role LD plays in solution.[57] By utilizing a double-mutant cycle, Cockroft et al.[57] extracted the interaction energy of alkyl chains (heptyl–hexyl) in multiple solvents. The study suggests a large compensation of LD in solution for linear alkyl chains and, instead, claims cohesive solvent interactions, i.e., solvophobic effects[80b,86] as the main driving force for aggregation. In a second study, Cockroft and co-workers focused on separating LD interactions from solvophobic effects using a perfluoroalkyl substituted balance.[60a] While a correlation with the cohesive energy density (ced) gave rise to the solvophobic effect, LD interactions were dissected using the bulk solvent polarizability. As a result, both effects were found to contribute to the dimerization of apolar alkyl groups with LD being more prominent in apolar organic and fluorous solvents. Pollice and Chen[87] investigated the intermolecular interactions of alkanes and perfluoroalkanes computationally (Figure 12). Whereas fluorinated substituents or molecules are generally argued to interact only weakly via LD interactions, the study pointed to the opposite. The computations showed that perfluorinated molecules such as tetrafluoromethane provide higher LD energy due to fluorine-fluorine contacts in comparison to the parent alkyl system. On the other hand, their conformational rigidity does not allow an ideal alignment thereby reducing the interaction energies. Interestingly, the origin of stabilization varies between alkyl-alkyl and fluorine-fluorine interaction. While LD stabilization originates from C–H bonding electron correlation of alkyl-alkyl contacts, fluorine-fluorine interactions are mostly generated by contacting fluorine atoms.[87]

As noted above, Chen et al.[19d] noticed a large compensation of inter- and intramolecular interactions in dichloromethane. Nevertheless, the effects of LD on the dissociation energies were not completely overridden by solute-solvent interactions. Further studies[53] of the same group focused on polar and nonpolar aprotic solvents. A comparison between experimental and computational data showed that implicit solvent models utilized to verify the observed trends underestimate solvent effects significantly. Apart from thermodynamic compensation, kinetic investigations on the unfolding process of azobenzenes substituted with increasingly longer alkyl chains contradict the sentiment that LD does not play a major role in solution. Wegner et al.[54b,c,88] identified alkyl–alkyl contacts in transition structures to be the dominant source of stabilization in the thermal equilibration of azobenzene switches, which can also be considered molecular balances. By utilizing unsymmetrically substituted azobenzene derivatives, Wegner et al.[89] demonstrated the decisive role of LD in stabilizing the (Z)-isomer via aryl-alkyl interactions. In contrast, the electronic structures of the aryl moieties were found to be negligible for isomerization. Additionally, the Wegner group introduced surface tension of the solvent as a key parameter that influences Z- to E-isomerizations.[88]

In 2021, Schreiner and co-workers[19e] revisited the cyclooctatetraene molecular balance to investigate solvation

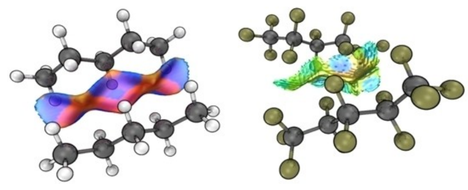

Figure 12. Strong LD and repulsive interactions between an *n*-pentane dimer (left) and the corresponding perfluorinated dimer (right). Due to a lack of flexibility, the perfluorinated dimer cannot exploit the full LD strength. Adapted from Pollice and Chen.[87]

effects on the equilibrium of the folded and unfolded diastereomer (Figure 13). The equilibrium of 1,4- and 1,6-COT is highly affected by the nature of the substituents attached.[70,73] Since only the folded conformer benefits from attractive LD interactions, the equilibrium counterintuitively shifts towards more crowded and sterically more hindered 1,6-COT. Modern computational methods, e.g., symmetry adapted perturbation theory[90] (SAPT), can be utilized to predict DED strength. Accordingly, the rigid dimer scan of the substituent distance in 1,6-COT (Figure 13) predicts the ideal ratio of LD and Pauli repulsion at a distance of around 2.5 Å.[19e] Remarkably, even though LD affects enthalpy and entropy, the two terms typically change in opposite directions so that the overall free energy changes little over the entire range of solvents of very different polarizabilities (Figure 14). Importantly, the sterically more demanding folded diastereomer is preferred in *all* solvents. Whereas hexane and cyclohexane diminish the interaction energy between both *tert*-butyl groups, quite polar solvents such as DMSO and DMF shift the equilibrium towards the folded diastereomer. In a follow-up, Bistoni, Schreiner and co-workers[91] focused on *n*-alkyl groups of varying size as solvents. Additionally, extremely bulky adamantyl and diamantyl substituents were utilized as DEDs. Despite their size, the more crowded 1,6-COT is *always* favored in solution.

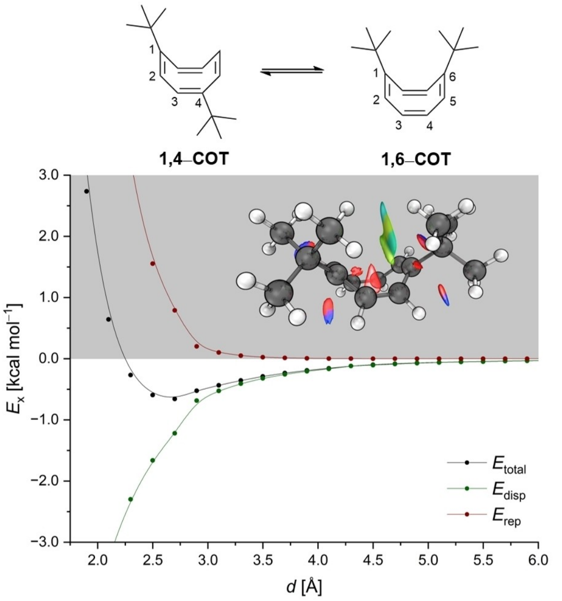

Figure 13. SAPT0/6-311G(d,p) energy decomposition of a scan of a rigid isobutane dimer. The non-relaxed dimer scan is based on the geometries of 1,6-COT. Every data point within the shaded area marks repulsive interactions. Adapted from Schreiner et al.[19e]

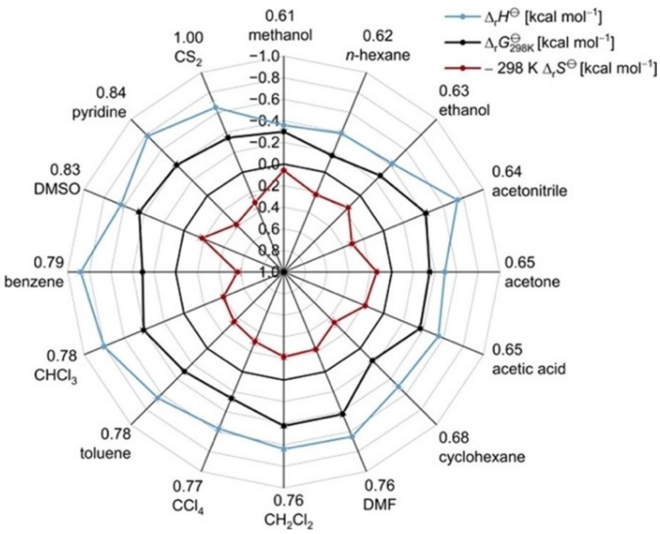

Figure 14. Correlation of thermodynamic quantities at 298 K in kcal mol^{-1} with clockwise increasing relative solvent polarizabilities (min = 0.00 vacuum, max = 1.00 CS_2). Reprinted with permission from Schümann et al..[19e] Copyright 2021 American Chemical Society.

3. London Dispersion as a Design Element for Unusual Molecular Structures

One of the most striking examples demonstrating the role LD plays in stabilizing structures is the counterintuitive case of hexaphenylethane (HPE).[12c] The unsubstituted HPE initially suggested by Gomberg[12a,92] dissociates into monomeric triphenyl methyl radicals and recombines to the well-known quinoid structure.[93] Understandably, steric hindrance between the phenyl moieties was taken as the origin for the very facile dissociation of HPE, which was considered unattainable.[94] Counterintuitively, sterically much more crowded all-*meta tert*-butyl HPE can be isolated (Figure 15).[12c,e,95] LD was found to be the origin of stability outweighing Pauli exchange repulsion by forming an LD stabilized "corset" of *tert*-butyl groups surrounding the labile central C–C bond (Figure 16).[12b,13] Accordingly, alkyl substitution was utilized to study the balance between attraction and repulsion not only in HPE but also in the head-to-head dimer of triphenylmethane both in the solid state and in the gas phase.[96]

Extending the central bond by using higher tetrel derivatives results in stable HPE-like compounds.[12f] While the central C–C bond (computed to be around ≈1.70 Å[12e]) of unsubstituted HPE is too short and Pauli exchange repulsion dominates, a more favorable ratio of repulsion vs. LD was found in higher tetrel congeners, where even unsubstituted phenyl moieties are sufficiently strong DEDs. This contradicts the (physically unfounded beyond diatomics) concept that longer bonds are weaker and dissociate more readily, because higher tetrel HPE derivatives form remarkably stable compounds due to strong LD interactions.[12f]

A similar bond stabilization can be utilized to connect bulky adamantyl moieties and circumvent dissociation via numerous attractive LD contacts. For instance, the resulting alkyl-alkyl contacts between diamondoids are sufficiently strong to yield exceptionally long central C–C bonds (≈1.71 Å) in diamondoid dimers.[13b,97] A combination of

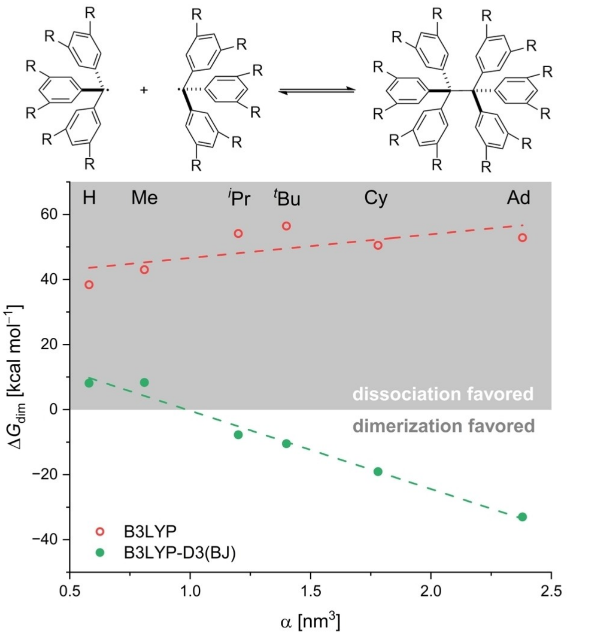

Figure 15. Dimerization energies ΔG_{dim} of all-*meta* substituted triphenyl methyl radicals including (green markings) and excluding (red markings) LD interactions. Note that only by including LD the HPE-like radical dimerization can be rationalized. Adapted from Rummel et al.[12e]

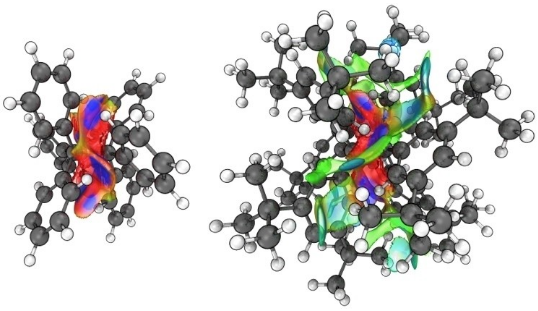

Figure 16. NCI plots of unsubstituted hexaphenylethane (left) and the *tert*-butyl substituted derivative (right). While the parent systems is strongly affected by repulsion (red isosurfaces), the substituted derivative benefits from stabilizing LD contacts (green isosurfaces). Adapted from Rummel et al.[12e]

single-crystal X-ray diffraction, gas-phase electron diffraction, combined GED/microwave (MW) spectroscopy, as well as quantum chemical computations confirmed the remarkable C–C bond lengths in the covalently bound diamantyl and oxadiamantyl dimers in the solid and in the gas phase.[98] Recently, Suzuki et al.[99] synthesized a hexaphenylethane-type hydrocarbon consisting of a central intramolecular C–C bond length of 1.77 Å. By utilizing bulk *tert*-butyl groups they observed a bond *contraction* due to close LD contacts. In marked contrast to the expected structural consequences of steric repulsion, the bulky substituents pull both molecular fragments together and prohibit bond dissociation. As for intramolecular stabilization, intermolecular dimerization of triphenylmethane derivatives benefits from the same interactions. While unsubstituted triphenylmethane dimerizes in a head-to-tail fashion, the all-*meta tert*-butyl derivative enforces a head-to-head structure yielding an incredibly short H–H contact ($\approx$1.57 Å). Although such a short intermolecular contact (the shortest on record to date in the Cambridge Crystallographic Data Centre) entails significant Pauli repulsion, an energy decomposition analysis reveals LD as the origin of stabilization (up to $E_{disp} = -52$ kcal mol^{-1}).[96a]

Even though LD is the dominant stabilizing factor in molecular (hydrocarbon) crystals, the observed triphenylmethane derivative dimer structures prevail in the gas phase as shown by ionization loss stimulated Raman spectroscopy in molecular beam experiments.[96b] Recently, the knowledge gained from such studies was utilized to enhance the interaction energies between amine-borane frustrated Lewis pairs (FLPs) to generate a crystalline encounter complexes. Accordingly, N(3,5-^{t}Bu$_2$C$_6$H$_3$)$_3$ and B(3,5-^{t}Bu$_2$C$_6$H$_3$)$_3$ were mixed and crystallized with the aim to stabilize the heterodimer of the encounter complex. While LD supports dimerization not only for heterodimer (N(3,5-^{t}Bu$_2$C$_6$H$_3$)$_3$/B(3,5-^{t}Bu$_2$C$_6$H$_3$)$_3$) formation but also for the homodimer (N(3,5-^{t}Bu$_2$C$_6$H$_3$)$_3$/N(3,5-^{t}Bu$_2$C$_6$H$_3$)$_3$ as well as B(3,5-^{t}Bu$_2$C$_6$H$_3$)$_3$/B(3,5-^{t}Bu$_2$C$_6$H$_3$)$_3$), no distinct characterization of an encounter complex has been reported.[100]

Apart from very bulky substituents the LD fingerprint can already be detected spectroscopically studying the aggregation of small molecules. In a multi-pronged spectroscopic approach, Gerhards et al. investigated the structural preferences of diphenyl ether–alcohol aggregates to bind via OH–O or OH-π interactions (Figure 17).[101] In a series of publications, a counterintuitive trend that larger alcohols favor OH–O arrangement was rationalized by accounting for LD and a deformation of the ether structure upon aggregation. Interestingly, by altering the flexibility of the ether by utilizing dibenzofuran as a rigid docking site, the trends reverse and OH-π interactions are favored for bulky alcohols.[102]

Utilizing rotational spectroscopy Schnell et al.[103] investigated the dimerization of dibenzofuran, diphenylether, and fluorene. With 60–70 % of the total interaction energy, LD was identified as the main driving force for molecular aggregation of all dimers. The aggregation of alcohols of increasing size with diadamantyl ether showed a competition of electrostatically and LD driven dimerization. Whereas water prefers hydrogen bonding resulting in close OH•••O bond distances governed by electrostatic interactions, bulk-

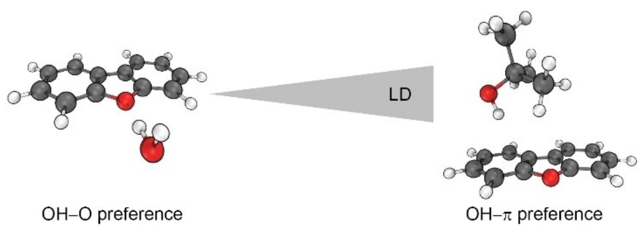

Figure 17. Preferred binding motif from oxygen-bound to π-bound structures with increasing solvent size.[102]

ier alcohols such as *tert*-butanol sacrifice electrostatic stabilization by maximizing LD contacts.[104] As a result, the OH•••O hydrogen bond distance increases with the number of close *tert*-butyl-adamantyl contacts.[105] The same method was applied to study the impact of fluorination in aromatic-diadamantyl ether aggregates via rotational spectroscopy.[106] In the same way, fluorinated benzene is expected to significantly alter its binding mechanism towards diadamantyl ether. As a matter of fact, the exchange of one hydrogen with fluorine is sufficient to change the preferred docking site of the benzene derivative with the diadamantyl ether. SAPT investigations demonstrate that in contrast to the common notion that fluorine is a poor DED, LD is always the main driving force for aggregation (around 70 % of the total interaction energy).

Suhm and co-workers[107] utilized a variety of spectroscopic tools to investigate the role of LD in dimerization and aggregation processes. In general, LD was found to be essential to determine the correct dimer geometries of molecules such as cyclohexanediol,[108] benzyl alcohols,[109] and *trans*-N-methylacetamide.[110] In addition, the docking preferences of alcohols and ketones were studied in supersonic jet expansion experiments and by measuring their spectroscopic signatures.[111]

In line with the HPE case, LD has been more appreciated as an additional source of stabilization for labile complexes and otherwise unstable molecules.[5,112] Initially, the "corset effect" was introduced to account for stabilizing interactions between steric bulk based on a "protective shell" around a reactive center. In this way, the synthesis of tetra-*tert*-butyltetrahedane was accomplished.[13a] Bulky *tert*-butyl groups successfully stabilize the tetrahedrane molecule as well as silyl groups due to a "protective LD shell".[13b,14,113] Recently, Cummins et al.[114] attributed the remarkable stability of the bulky phosphatetrahedranes ($(^tBuC)_3P$) to a network of close H···H contacts.[115] The accompanying computational study revealed a total of nine H···H contacts with a stabilizing effect of $-0.7\ \text{kcal mol}^{-1}$ per contact due to LD.[114]

While such H···H contacts counteract the ring strain of tetrahedrane, *tert*-butyl substituents are usually utilized to introduce steric hindrance. In an attempt to quantify steric effects experimental parameters like the Winstein-Holness A-values[116] were introduced to define steric hindrance. Based on the ratio of axial *vs.* equatorial monosubstituted cyclohexane, the A-value (the negative of the free energy change of this equilibrium) is sensitive to destabilizing contacts in the axial position. Recently, the experimental data were revisited computationally with the goal to conceptualize a DED scale.[76c] Whereas steric bulk is the factor defining the thermodynamic stability of monosubstituted cyclohexane derivatives, LD was found to play a non-negligible part to rationalize the experimental data (Figure 18) that are at odds with the originally proposed A-values. This is particularly apparent for the counterintuitive A-values of pinacol boronic acid (Bpin) and glycol boronic acid (Bgly).[117] While Bpin (A-value of $0.42\ \text{kcal mol}^{-1}$) is clearly the smaller substituent in comparison to Bgly (A-value of $0.73\ \text{kcal mol}^{-1}$), it disfavors the axial position more

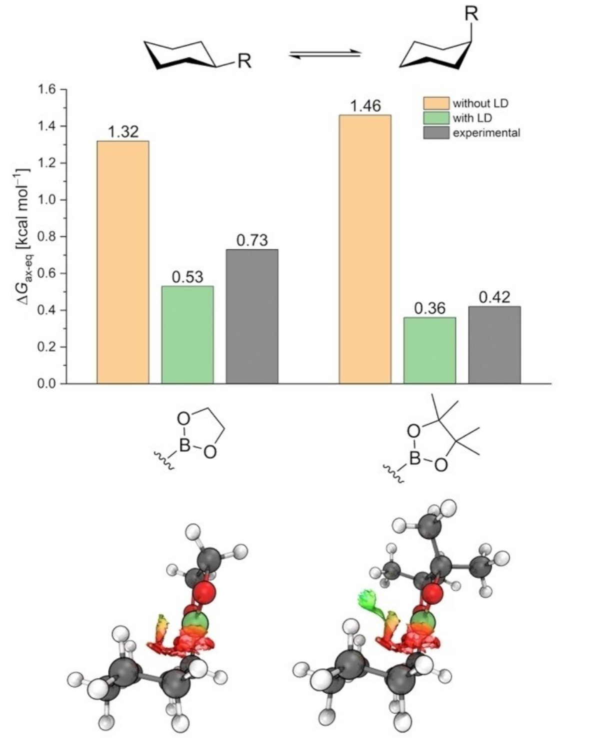

Figure 18. Computed and experimental $\Delta G_{\text{ax-eq}}$ (A-values) for pinacol boronic acid (right) and glycol boronic acid (left) substituted cyclohexane derivatives (top). The corresponding NCI plots (bottom) visualize noncovalent interactions. Note that the experimental data can only be reproduced computationally upon including LD. Adapted from Solel et al.[76c]

than the much larger Bgly. In contrast to Bgly, Bpin benefits from additional H···H contacts stabilizing the axial conformer due to LD. Apart from alkyl contacts, halogen-alkyl and halogen-halogen interactions were identified to be valuable DEDs influencing the landscape of potential energy surfaces significantly.[76c,118]

4. London Dispersion as a Driving Force for Reactivity and Catalysis

Since LD interactions significantly influence the conformational landscape of molecules and can be used as thermodynamic driving force for chemical reactions, it becomes apparent that these manifestations can be transferred to catalytic processes as well. In the field of catalysis, the rather incomplete concept of steric hindrance (by and large Pauli exchange repulsion) is commonly utilized.[119] The hard-sphere classical mechanics model is the basis for this oversimplification (and exclusion of quantum mechanics). While this might be true for some cases, most early studies on catalytic processes lacked a detailed analysis of the role of noncovalent attractive interactions. Although observations that steric crowding can enhance reaction rates and increase selectivities, this is often attributed to repulsive interactions. Since Pauli repulsion is always destabilizing, it cannot be the origin of increased reaction rates. Therefore, a balance between attractive and repulsive interactions must be operative and this realization can lead to improved catalysts. Stabilizing LD interactions in energy minima on a potential energy hypersurface can be directly transferred to transition structures as well.[7b,120]

Since LD interactions are ubiquitous and omnidirectional, not only productive reaction steps are promoted. This becomes apparent when catalytically inactive conformers of a catalyst are favored due to LD, thereby inhibiting catalysis. For instance, thiourea catalysis is based on substrate activation due to double hydrogen bonding of the unfolded (*anti-anti*) conformer of diphenylthiourea derivatives.[121] While this has been confirmed experimentally and computationally for *N*,*N'*-bis[3,5-bis(trifluoromethyl)phenyl]thiourea, the implementation of bulky electron-donating substituents in all-*meta* position inhibits catalysis.[121e] In a recent study, LD interactions were identified to shift the conformational preference of diphenylthiourea derivatives towards the sterically more crowded *syn-syn* conformer (Figure 19).[122] Systematic low-temperature NMR studies helped quantify the effects of LD on the equilibrium of *syn-syn* and *syn-anti* diphenylthiourea derivatives. Accordingly, the incorporation of bulky all-*meta-tert*-butyl substituents shifts the equilibrium towards the *syn-syn* conformer by around 1.7 kcal mol^{-1}. A double-mutant-cycle dissected the interaction energy between DEDs into stabilizing alkyl–alkyl contacts (around 30 % of the total interaction energy) and σ-π interactions between DED and the opposing phenyl moiety (70 %). The preference for the *syn-anti* and *syn-syn* conformers restricts effective catalytic processes.[122]

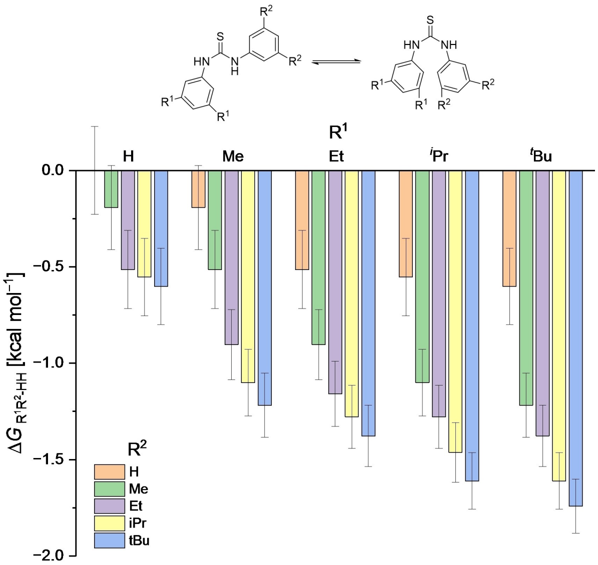

Figure 19. Gibbs free energy values for the equilibrium of *syn-syn* and *syn-anti* diphenylthiourea at 193 K substituted with DEDs in all-*meta* positions. $\Delta G<0$ corresponds to a shift towards the *syn-syn* conformer. Adapted from Rummel et al.[122]

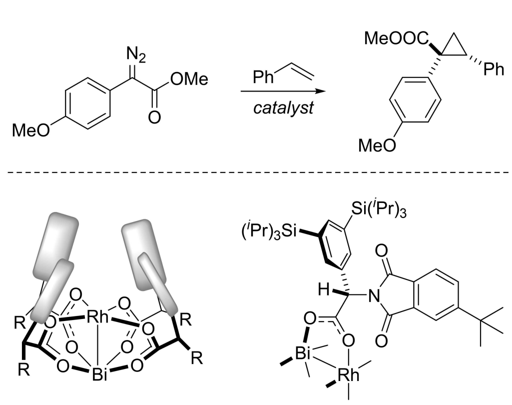

Figure 20. Cyclopropanation of styrene utilizing a herterobimetallic bismuth-rhodium paddlewheel complex. Adapted from Fürstner et al.[123a]

Whereas LD can reduce the catalytic activity of thiourea derivatives, the opposite effect is observed for a chiral bismuth-rhodium paddlewheel catalyst (Figure 20). By utilizing LD, Fürstner et al.[123] locked the chiral calyx of a bismuth-rhodium catalyst in place. A combination of TIPS and *tert*-butyl substituents stabilize the active catalyst conformer.[124] Computations reveal up to −11.6 kcal mol^{-1} stabilization due to LD, whereas the TIPS and *tert*-butyl butyl groups account for ≈32 % and ≈12 % respectively. A new generation of Rh–Bi catalysts outperformed the old ones regarding selectivity and reactivity. Whereas a cyclopropanation reaction using *N*-phthalimido substituents on the *tert*-leucine ligands gave full conversion in >3 h, the new set of ligands completed the reaction within 10 min with outstanding selectivity. Since the more sterically hindered catalyst proceeds with higher reaction rates, *stabilizing* LD interactions are attributed to the increase in reactivity.[123a]

Bistoni et al.[125] examined an asymmetric intramolecular hydroalkoxylation of terminal olefins catalyzed by bulky Brønsted acids.[126] By studying the conformational flexibility in the transition structure of the reaction, the interplay of catalyst and substrate was of capital importance. The authors observed a distortion of the catalyst to maximize the intermolecular interactions with the substrate. The energy penalty arising from conformational distortions was overwritten by a number of LD interactions.[125]

It is known that a detailed understanding of all catalyst-substrate interactions must be considered to rationalize catalytic activity. Whereas steric hindrance prevents close contact, LD interactions dominate aggregation of catalyst and substrate (and their competing homodimeric structures).[4a,120,127] Thus, rate acceleration can only be rationalized due to the presence of attractive (noncovalent) interactions. Selectivity, on the other hand, can be evoked by both, repulsive steric interactions decelerating the reaction toward one product and steric attraction[124,128] favoring the reaction to the other. Size-dependent rate acceleration was observed in competition experiments between secondary alcohols and silyl reagents of varying size (Figure 21). While silyl groups are commonly utilized to introduce steric bulk[75–76,77] and prohibit chemical reactions, Zipse et al.[129] observed a systematic rate increase of a silylation reaction using large DED substituents. In a combined experimental and computational study, Zipse and

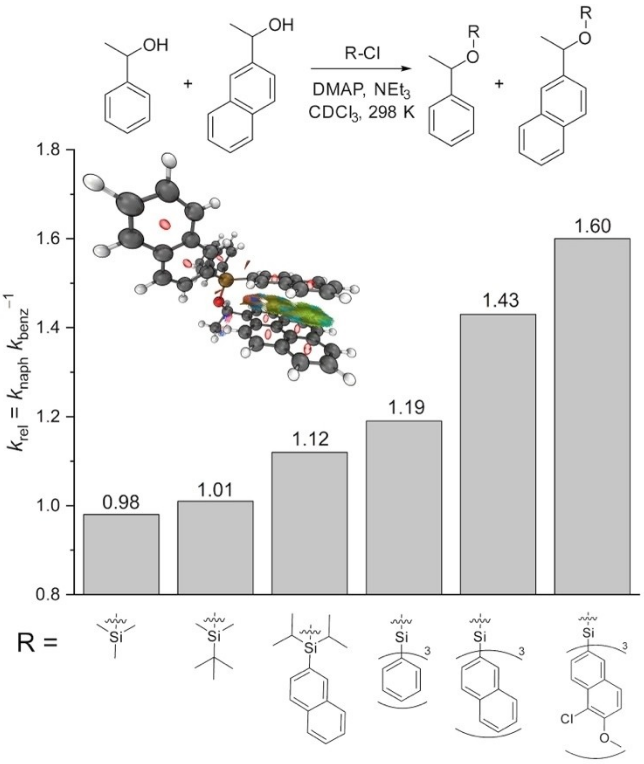

Figure 21. Relative rate constants k_{rel} for competition experiments between 1-phenylethanol and 1-naphthylethanol with increasingly larger silyl chlorides. The NCI plot highlights π-π (LD) interactions (green isosurface). Adapted from Zipse et al.[129]

co-workers isolated LD interactions as dominant factor for rate increase. Whereas small silyl reagents (e.g., TMSCl) do not provide a sufficient number of LD contacts, large aromatic substituents increase the reaction rates.

The same effect was taken advantage of in the kinetic resolution of secondary alcohols.[130] By utilizing chiral pyridine derivatives with increasingly larger aromatic side chains, the rate accelerated by a factor of up to 40. Computational investigations revealed that the most crowded transition structure was favored by around 1.6 $kcal\,mol^{-1}$ resulting in high kinetic selectivity factors ($s \geq 50$). The origin for the stabilization lies in attractive CH-π and π-π interactions. Accordingly, the concept of steric attraction[124,128] (via LD) was successfully utilized to increase reaction rates and improve enantioselectivities.[130]

The Corey-Bakshi-Shibata (CBS) reduction[131] of prochiral ketones is a striking example where stereoselectivity is explained solely on the basis of a classic steric repulsion model. The proposed (and widely accepted) mechanism for the enantioselective reduction of ketones by oxazaborolidines (OXB) is based on repulsive interactions[132] between the boron substituent R on the catalyst and the largest substituents R_L of the ketone. Repulsive interactions between R and R_L are designated as to disfavor the six membered boat-like transition state to the (*S*)-product, delivering the (*R*)-enantiomer with high selectivity. While this concept can qualitatively predict the enantioselectivities for many substrates, it fails for ketones such as 1-cyclopropyl-2-methylpropan-1-one.[132b]

Since both substituents are similar in steric size, poor selectivity would be predicted. Nevertheless, the (*R*)-enantiomer formed in 91 % *ee*. Schreiner et al.[4b] investigated the origin of this selectivity by questioning the steric repulsion argument and by including LD in the mechanistic and structural rationale. In contrast to Corey's model, the reactions are actually more selective upon removal of the large phenyl substituent on boron. Instead, LD interactions between the OXB carbinyl phenyl groups interact favorably with the substrate (Figure 22). With this improved mechanistic and more physically sound understanding of the CBS reduction (also including a boat-shaped transition structure) it was possible to modify the catalyst to show improved enantioselectivities even for the most challenging substrate butanone (Figure 23). This most difficult methyl-ethyl dis-

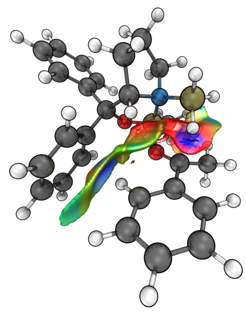

Figure 22. NCI plot of the lowest-lying transition structure for the reduction of acetophenone with OXB. Stabilizing CH-π interactions highlight the role of the phenyl moieties at the carbinyl position of OXB in the transition structure. Rather than steric hindrance they provide an anchor to hold the substrate in place via LD interactions. Adapted from Schreiner et al.[4b]

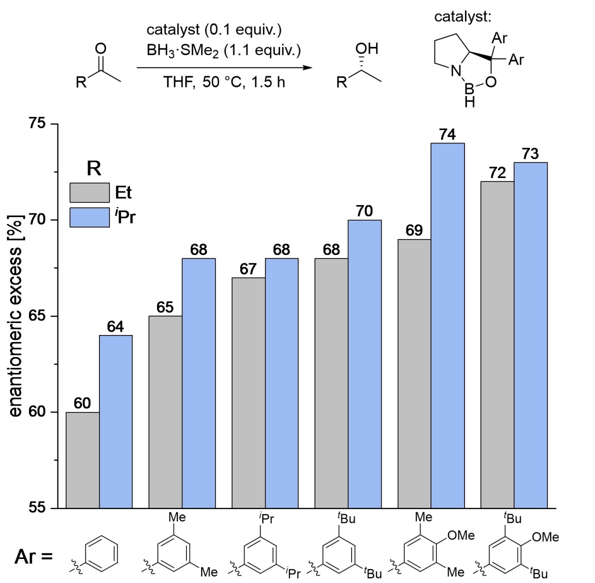

Figure 23. CBS reductions of butanone (grey) and 3-methyl-2-butanone (blue) employing modified catalysts of growing size. Adapted from Schreiner et al.[4b]

crimination in butanone improved from 60% ee to 72% ee with a DED-enhanced OXB catalyst.

Since LD interactions are additive and highly dependent on the number of short-range contacts, large molecules, such as peptides or the double helix of DNA, greatly benefit from LD.[133] Hobza and co-workers[134] as well as Bistoni et al.[135] demonstrated the importance of LD for the intrinsic stability of the duplex structure of DNA using advanced quantum mechanical methods. Even in the presence of multiple noncovalent contacts, LD is essential for the stability of such large molecular structures.

Catalysis with short peptides can also take advantage of LD. For example, in the enantioselective kinetic resolution of *trans*-cyclohexane-1,2-diols through monoacylation a non-natural oligopeptide catalysts was developed.[136] While the nucleophilic *N*-π-methylhistidine moiety is catalytically active and performs the enantioselective acyl transfer,[137] cyclohexylalanine was incorporated to act as a DED. Both, computational and experimental evidence suggest the formation of an enzyme-like pocket in which the substrate is bound via hydrogen bonding and LD interactions.[127b,138] The molecular aggregation due to LD was probed using advanced NMR methods.[127b] The investigations included a conformational analysis of the organocatalyst as well as the aggregation of substrate and catalyst via nuclear-Overhauser effect (NOE)-based NMR spectroscopy. As a result, the NOE-contacts between the substrate (*trans*-cyclohexane-1,2-diol) and the cyclohexyl moiety of the oligopeptide catalyst were observed.

Similar catalyst-substrate binding was exploited to develop the first enantioselective Dakin-West reaction (Figure 24).[127a] Due to achirality of two intermediates, stereoselective catalysis had been difficult to achieve for decades. While the oligopeptide catalyzes the Steglich rearrangement as well as the final decarboxylation and re-protonation, stereoselectivity was only realized in the last step. A combination of LD and enolate binding holds the substrate in place for stereoselective re-protonation of the terminal enol. Again, cyclohexyl groups proved most effective as DEDs due to their restricted flexibility and high polarizability (Figure 24). The same catalyst was also utilized in site-selective acylation of pyranosides.[139] LD is likely to bind the carbohydrate in the catalysts' pocket thereby facilitate site-selectivity.

In the Brønsted acid catalyzed transfer hydrogenation of imines, the incorporation of bulky DEDs significantly enhances enantioselectivies due to stabilization of the *Z*-imine transition state. Gschwind et al.[140] developed an LD-controlled catalytic cycle by investigating the impact of *tert*-butyl groups on the conformational preference of the starting material and the termolecular transition structure (Figure 25). Although the *E*-imine is in general the preferred isomer, sophisticated NMR techniques revealed a shift of the equilibrium between the *E*- and *Z*-imine to the more crowed *Z*-imine by around 1 $kcal\,mol^{-1}$. While the dimerization of starting material and catalyst significantly favors the *Z*-imine, the stabilizing effects of *tert*-butyl substituents prevail throughout the entire reaction process. This leads to a significant increase of enantioselectivity.

Chiral phosphoric acids were also used to achieve high enantioselecivities in, e.g., the Minisci reaction of alcohols. Phipps et al.[141] reported the first enantioselective Minisci reaction that uses α-hydroxy radicals instead of commonly employed α-amino radicals. Both, experimental and computational investigations point to a deprotonation as the selectivity- and rate-determining step with noncovalent interactions being responsible for enantiodiscrimination. While the formation of the major product is stabilized by LD between the substrate and 3,3′-substituents of the phosphate catalyst, the transition structure of the minor product lacks such stabilization. The consideration of LD in the computational analysis led to excellent agreement of

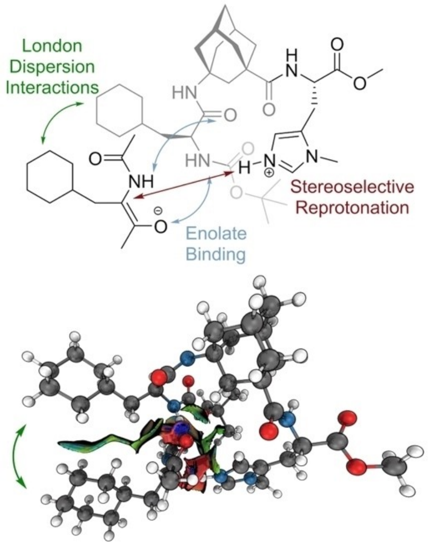

Figure 24. Association of protonated catalyst and substrate in the first enantioselective Dakin-West reaction. The NCI plot highlights the importance of attractive alkyl-alkyl contacts anchoring the substrate in the catalyst's pocket. Adapted from Wende et al.[127a]

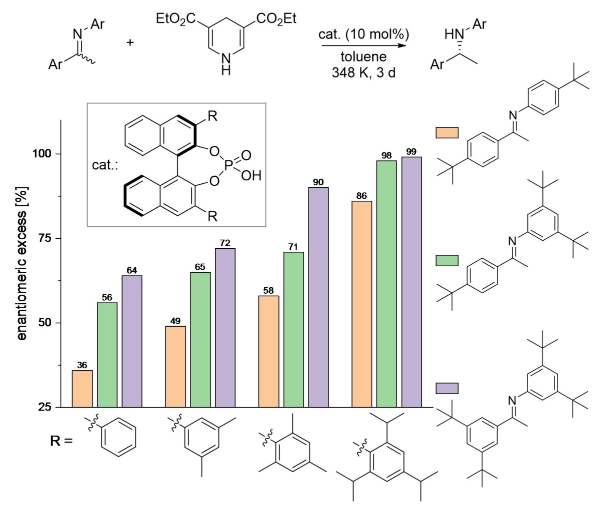

Figure 25. Enantioselectivities for the transfer hydrogenation of imines utilizing *tert*-butyl groups for efficient catalyst-substrate binding. Adapted from Gschwind et al.[140]

experimental and computational data. Toste et al.[127c] studied an enantioselective allenoate-Claisen rearrangement using chiral phosphoric acid catalysts. Upon coordination to a sodium cation a catalytic pocket formed that maximizes noncovalent interactions. Since phosphoric acid catalysts can readily be substituted, they might benefit greatly from LD interactions.

Studying bioorthogonal reactions Franzini and co-workers[142] noticed an unexpected rate increase in the cycloaddition of 3,6-dialkyl-tetrazines and (2-isocyanoethyl)benzene by introducing steric bulk (Figure 26). Accordingly, the introduction of *tert*-butyl groups at the tetrazine increased the reaction rate by a factor of eight. Since repulsive interactions cannot be responsible for rate increases, LD interactions were studied in detail. A computational analysis revealed increasing LD interactions (≈ -6.0 kcal mol^{-1}) in the rate-determining transition structure with increasing steric bulk for the reaction with isonitriles. Due to the linear structure of the isonitrile group steric hindrance was estimated to be minimal (≈ 1.0 kcal mol^{-1}).

To efficiently use attractive noncovalent interactions in catalysis, substrate and catalyst need to be geometrically compatible with each other.[143] While this compatibility is usually achieved by utilizing functional groups, Karton et al.[144] recently demonstrated that simple pristine graphene catalyzes the racemization chiral 1,1′-binaphthyl-2,2′-diol (BINOL) via large area noncovalent contacts. By utilizing a single-layer graphene (*R*)-BINOL ($>99{:}1$ *e.r.*) could be completely racemized. Computations showed that a combination of LD and electrostatic interactions (with the former being more prominent) is the basis for catalytic activity. Similar effects were observed for the bowl-to-bowl inversions of corannulene and sumanene using graphene and h-BN as catalysts.[145]

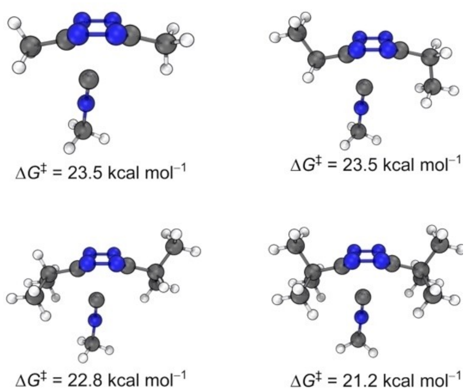

Figure 26. Computed structures and Gibbs free energies of the transition structure of the model reaction of substituted tetrazines with methylisonitrile. Adapted from Franzini et al.[142a]

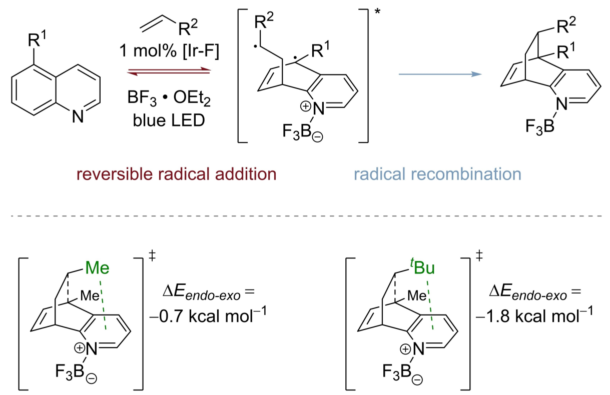

Figure 27. Photochemical reaction of a quinolone derivative with an alkene (top). Selectivity determining transition structure (bottom) with methyl and *tert*-butyl substituents. Adapted from Brown et al.[146]

The stereo- and regiochemical outcomes of photochemical dearomative cycloadditions were found be significantly influenced by LD. Brown and co-workers reported a cycloaddition of quinoline derivatives with alkenes proceeding via a stepwise radical reaction (Figure 27).[146] After initial reversible radical addition the *endo* product formed preferably in a selectivity determining radical recombination. Accordingly, the more sterically demanding product forms; this is also true for the extremely bulky adamantyl substituent. Computational investigations found LD to be decisive for selectivity. A comparison between dispersion corrected functionals and those excluding LD demonstrated that only by including LD the selectivity was reproduced. Thus, methyl substitution favors the *endo* transition structure by -0.7 kcal mol^{-1}. Additionally, σ-π interactions increase with steric bulk favoring the *endo* reaction path by -1.8 kcal mol^{-1} with *tert*-butyl substitution.[146]

In the field of transition-metal catalysis, electronic and steric arguments (as if they were separable!) are commonly utilized to rationalize ligand effects.[147] While the first is described as a through-bond[148] effect, bulky substituents in the periphery of the metal center mostly affect the catalyst-substrate through-space interactions.[120,149] Both effects greatly influence the catalytic performance by altering rate determining transition structures. Typically, the through-space interaction is described as steric repulsion.[150] This argument effectively rationalizes an increase in selectivity due to repulsive interactions by shielding certain parts of the metal catalyst. However, the notion that higher steric bulk, i.e., a *destabilization* by definition, increases reaction rates must be called into question.

Naturally, LD interactions can override steric repulsion due to a large number of attractive ligand-substrate contacts.[151] Nevertheless, attractive noncovalent interactions are rarely discussed in transition-metal catalysis even though a ligand that is able to attractively interact with a substrate is crucial for reactivity and selectivity.[112,152] While systematic studies of LD effects on organic reactions or structures are feasible, polarized metal centers prove difficult when it comes to dissecting between various noncovalent interactions. For instance, a thorough analysis of through-space interactions was performed for a copper-catalyzed hydroamination reaction of unactivated olefins by Liu et al.[4a] The reaction proceeds via a hydrocupration onto the olefin as the rate determining step. Whereas commonly utilized ligands, such as SEGPHOS, hardly catalyze the reaction for unactivated substrates, the introduction of bulky *tert*-butyl substituents counterintuitively increases reaction rates and yields. Liu et al.[4a] utilized a ligand-substrate interaction model to dissect the through-bond and -space interactions into the main contributors to the activation barrier (Figure 28). *Via* a combination of experimental and computational investigations, they identified LD interactions to be the dominant factor in the transition structure of the reaction. By incorporating bulky di-*tert*-butyl-methoxy (DTBM) substituents, the substrate scope and reactivity increased significantly. In a later study, the catalysts' performance in a hydroboration reaction was further increased by exchanging bulky *tert*-butyl substituents with higher tetrel congeners.[17] By utilizing trimethylsilyl (TMS) and trimethylgermanium (TMG) as DEDs the interactions between the catalyst and substrates was further optimized resulting in higher yields and faster reactions. Thereby, the incorporation of higher tetrels enhances LD interactions between catalyst and substrate due to their increased size and polarizabilities. A similar effect is responsible for the observed stability of higher tetrel hexaphenylethane congeners, whereas the original carbon-based hexaphenylethane has not been prepared to date (see above).[12f] Other studies also indicate that silyl groups can be utilized as DEDs despite their large steric demand.[18,75,129–130,153] Similar to the SEGPHOS ligand, prolinol-phosphine ligands bearing DTBM groups were successfully utilized in silver catalyzed asymmetric aldol reactions as decisive structural features for stereoselectivity. Computational investigations point to a combination of non-classical C–H···O hydrogen bonding and LD interactions stabilizing the rate-determining transition structure.[154]

In 2018, Sawamura et al.[155] introduced the copper-catalyzed asymmetric alkynylation of α-ketoesters. A combination of hydrogen bonding and LD interactions between the chiral phosphine ligand and substrate was identified as the origin for the observed enantioselectivities. Apart from transition state stabilization, LD interactions significantly

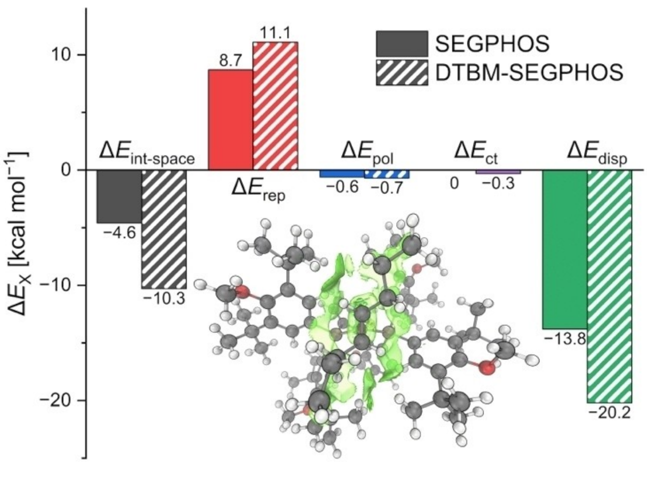

Figure 28. Energy decomposition analysis of the ligand-substrate interaction energies in the transition structure of the hydrocupration reaction of *trans*-4-octene reacting with SEGPHOS (bold markings) and DTBM-SEGPHOS (striped markings). Adapted from Liu et al.[4a]

alter the reactions' energy profile. Computations of the Cobalt-catalyzed C–H cyanation reaction show that, both, energy barriers and minima are stabilized by LD.[156] Here, the Cp* ligand was utilized to interact as DED and stabilize labile complexes with the Co catalyst. An LED analysis revealed strong LD interactions of up to 12 kcal mol^{-1} between the CP* ligand and the substrate. Consequently, the CP* ligand does not interact via steric shielding but rather stabilizes the complex due to CH-π contacts.[157] Similar effects were reported for a Mn-catalyzed C–H-bond functionalization.[158] LD was computed to play a dominant role in stabilizing the key transition structures. As a consequence, the role of bulky ligands[159] in transition metal catalysis should be carefully considered and re-evaluated. The non-innocence of steric bulk can usually be traced back to a fine interplay of Pauli repulsion and LD in enantioinduction.[160] A similar effect was recently reported by Knowles et al.[161] studying a catalytic asymmetric hydrogen atom transfer reaction. Here, LD as well as hydrogen-bonding and π-π stacking were reported to be origin for substrate recognition and enantioinduction.

Accordingly, in the developing field of dual transition metal catalysis noncovalent interactions have begun to move into the spotlight. Here, LD is utilized as a tool to enable face-selectivity via π-π interactions.[162] Pursuant to this, Rios et al.[163] reported an enantioselective synthesis of dihydroacridines utilizing LD as the key attractive interaction stabilizing the rate determining step. In the zirconocene catalyzed ethylene polymerization, Ess and co-workers computationally investigated the role of LD during α-olefin co-monomer incorporation. Both fields largely use the concept steric hindrance rather than attractive noncovalent interactions. Counterintuitively, they identified LD as decisive factor for selectivity and incorporated LD as a ligand design feature.[164]

Whereas chemical reactions can benefit from LD interactions due to lower energy barriers in the rate determining step, LD can also help in elucidating mechanisms of catalytic processes. Berkessel and co-workers[165] utilized bulky 2,6-bis(2-propyl)phenyl (Dipp) and 2,4,6-trimethylphenyl (Mes) substituents attached to *N*-heterocyclic carbenes to stabilize and characterize the elusive Breslow intermediate. Computations suggest LD to be the major component of the thermodynamic stability of the intermediate.

While LD can be regarded as the key interaction to stabilize metal-NHC[112,166] complexes, the selectivity of such catalysts was studied experimentally and computationally with respect to the role of noncovalent interactions in the rate determining transition state.[167] A ruthenium catalyst bearing NHC ligands can be utilized for enantioselective hydrogenation of heteroarenes to generate saturated heterocycles.[168] The corresponding mechanism consists of a hydride and a subsequent proton shift with the first being rate determining. Enantioselectivity is determined by substrate coordination via the *re* or *si*-face of the substrate. Glorius et al.[168] located a decisive structural feature for binding of the substrate which affects the energy of all subsequent reaction steps. While *re*-face coordination is dominated by a flat interaction surface of the catalyst and

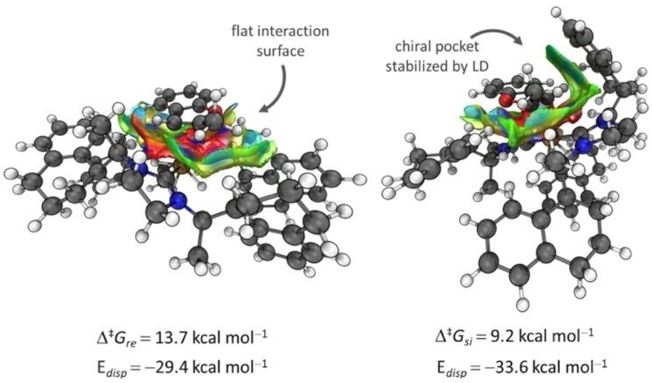

Figure 29. NCI plot and computed energies of the rate determining transition structure of the ruthenium NHC-catalyzed asymmetric heteroarene hydrogenation. The *si* transition structure (right) results in major enantiomer. Adapted from Glorius et al.[168]

while there is no steric hindrance, a more crowed catalyst-substrate complex forms via *si*-face coordination (Figure 29). Still, *si*-face coordination yields the major enantiomer. In line with the induced fit model,[169] the catalyst bends around the substrate and forms a pocket by maximizing LD interactions. While this pocket cannot form upon *re*-face coordination, LD stabilizes the more hindered pathway. With a difference in Gibbs free energy of the transition structure of 1.9 kcal mol^{-1} (experimentally determined) the reaction yields the (*R*)-configured product with 96:4 *e.r.*[168] Similar effects were observed by Bistoni et al.[170] who computationally assessed the mechanism and stereoselectivities of asymmetric catalytic Diels–Alder reactions. LD was found to be an indispensable feature of catalyst-substrate aggregation.

The role of NHC ligands as the origin for additional stabilization via LD has also been taken advantage of in hydroarylation reactions of unactivated alkenes. Very bulky and highly substituted NHCs and a nickel catalyst were demonstrated to increase reactivities and selectivities due to a combination of LD and electrostatic interactions.[171]

Comparable impact of LD was reported for the Pd catalyzed stereoselective synthesis of tetrasubstituted chromanones. The chiral pyridine-dihydroisoquinoline ligand (PyDHIQ) utilized to induce excellent stereoselectivities consists of a floppy benzyl group substituted with steric bulk to make use of steric hindrance as a directing effect.[172] Andreola and Wheeler[173] computationally found stabilizing hydrogen bonding and LD interactions as the main origin for observed selectivities. Accordingly, the floppy benzyl substituent at PyDHIQ favors a closed conformation in the transition structure, thereby interacting with the substrate.

5. Conclusions

LD interactions are ubiquitously present in all areas of chemistry. Nevertheless, the "steric hindrance model and explanations" are still ubiquitously used as it is often assumed that LD interactions are negligible in comparison to polar interactions and are largely outweighed by Pauli repulsion. With the large body of evidence accumulated over the last decade in favor of considering LD, this review hopefully demonstrates that these interactions can overall be large and must be considered when discussing structure, reactivity, catalysis, and spectroscopy.

In the recent years, great progress has been made in quantifying and hence understanding LD interactions. DEDs are now regularly used to influence structural stability or enforce selectivity. Especially labile and highly reactive molecules benefit from LD and can now be studied in unprecedented detail.

In catalysis, the fine interplay of LD and Pauli repulsion between catalyst and substrate is chiefly responsible for reactivity and selectivity. Accordingly, fine-tuning the ratio of LD and repulsive interactions greatly affects catalyst activity and selectivity.

By reconsidering the interplay of attractive and repulsive interactions, new limits for molecular binding situations, chemical reactions, selectivites, and structural motifs can be set. While the currently most common way of thinking about structures and molecular interactions is based on repulsive interactions, the inclusion of attractive LD allows to exceed such chemical restrictions and expands our possibilities.

Acknowledgements

This work was supported by the priority program "Control of London Dispersion in Molecular Chemistry" (SPP1807) of the Deutsche Forschungsgemeinschaft. With the end of the program, we thank all principal investigator contributing for a successful collaboration. We thank Jan M. Schümann for fruitful discussions. We are grateful to Elisa Monte for designing the cover art. Open Access funding enabled and organized by Projekt DEAL.

Conflict of Interest

The authors declare no conflict of interest.

Data Availability Statement

Data sharing is not applicable to this article as no new data were created or analyzed in this study.

Keywords: Molecular Balance · Noncovalent Interactions · Spectroscopy · Structure and Reactivity · van der Waals Forces

[1] a) J. D. van der Waals, *Over de Continuiteit van den Gas-en Vloeistoftoestand, Vol. 1*, Sijthoff, **1873**; b) J. D. van der Waals, *Die Continuität des gasförmigen und flüssigen Zustandes*, J. A. Barth, Leipzig, **1881**; c) J. D. van der Waals, J. S. Rowlinson, *On the continuity of the gaseous and liquid states*, Courier Corporation, **2004**; d) K.-T. Tang, J. P. Toennies, *Angew. Chem. Int. Ed.* **2010**, *49*, 9574–9579.

[2] A. Stone, in *Molecular Liquids*, Springer, Berlin, **1984**, pp. 1–34.
[3] H.-J. Schneider, *Angew. Chem. Int. Ed.* **2009**, *48*, 3924–3977.
[4] a) G. Lu, R. Y. Liu, Y. Yang, C. Fang, D. S. Lambrecht, S. L. Buchwald, P. Liu, *J. Am. Chem. Soc.* **2017**, *139*, 16548–16555; b) C. Eschmann, L. Song, P. R. Schreiner, *Angew. Chem. Int. Ed.* **2021**, *60*, 4823–4832.
[5] D. J. Liptrot, P. P. Power, *Nat. Chem. Rev.* **2017**, *1*, 0004.
[6] a) W. Heitler, F. London, *Z. Phys.* **1927**, *44*, 455–472; b) F. London, *Z. Phys. Chem. Abt. B* **1930**, *B11*, 222–251; c) F. London, *Z. Phys.* **1930**, *63*, 245–279; d) R. Eisenschitz, F. London, *Z. Phys.* **1930**, *60*, 491–527.
[7] a) R. Warmuth, J.-L. Kerdelhué, S. Sánchez Carrera, K. J. Langenwalter, N. Brown, *Angew. Chem. Int. Ed.* **2002**, *41*, 96–99; b) J. P. Wagner, P. R. Schreiner, *Angew. Chem. Int. Ed.* **2015**, *54*, 12274–12296.
[8] a) F. London, *Trans. Faraday Soc.* **1937**, *33*, 8b–26; b) J. N. Israelachvili, in *Intermolecular and Surface Forces (Third Edition)* (Ed.: J. N. Israelachvili), Academic Press, San Diego, **2011**, pp. 107–132.
[9] D. G. Truhlar, *J. Chem. Educ.* **2019**, *96*, 1671–1675.
[10] K. S. Pitzer, E. Catalano, *J. Am. Chem. Soc.* **1956**, *78*, 4844–4846.
[11] S. Grimme, R. Huenerbein, S. Ehrlich, *ChemPhysChem* **2011**, *12*, 1258–1261.
[12] a) M. Gomberg, *Ber. Dtsch. Chem. Ges.* **1900**, *33*, 3150–3163; b) S. Grimme, P. R. Schreiner, *Angew. Chem. Int. Ed.* **2011**, *50*, 12639–12642; c) S. Rösel, P. R. Schreiner, *Isr. J. Chem.* **2022**, *62*, e202200002; d) S. Rösel, J. Becker, W. D. Allen, P. R. Schreiner, *J. Am. Chem. Soc.* **2018**, *140*, 14421–14432; e) S. Rösel, C. Balestrieri, P. R. Schreiner, *Chem. Sci.* **2017**, *8*, 405–410; f) L. Rummel, J. M. Schümann, P. R. Schreiner, *Chem. Eur. J.* **2021**, *27*, 13699–13702.
[13] a) G. Maier, S. Pfriem, U. Schäfer, R. Matusch, *Angew. Chem. Int. Ed.* **1978**, *17*, 520–521; b) P. R. Schreiner, L. V. Chernish, P. A. Gunchenko, E. Y. Tikhonchuk, H. Hausmann, M. Serafin, S. Schlecht, J. E. P. Dahl, R. M. K. Carlson, A. A. Fokin, *Nature* **2011**, *477*, 308–311.
[14] G. Maier, J. Neudert, O. Wolf, D. Pappusch, A. Sekiguchi, M. Tanaka, T. Matsuo, *J. Am. Chem. Soc.* **2002**, *124*, 13819–13826.
[15] a) S. Ndambuki, T. Ziegler, *Inorg. Chem.* **2012**, *51*, 7794–7800; b) I. Seidu, M. Seth, T. Ziegler, *Inorg. Chem.* **2013**, *52*, 8378–8388.
[16] S. Paliwal, S. Geib, C. S. Wilcox, *J. Am. Chem. Soc.* **1994**, *116*, 4497–4498.
[17] Y. Xi, B. Su, X. Qi, S. Pedram, P. Liu, J. F. Hartwig, *J. Am. Chem. Soc.* **2020**, *142*, 18213–18222.
[18] L. Rummel, H. F. König, H. Hausmann, P. R. Schreiner, *J. Org. Chem.* **2022**, *87*, 13168–13177.
[19] a) C. A. Hunter, *Angew. Chem. Int. Ed.* **2004**, *43*, 5310–5324; b) K. D. Shimizu, *Nat. Chem.* **2013**, *5*, 989–990; c) J. W. Hwang, B. E. Dial, P. Li, M. E. Kozik, M. D. Smith, K. D. Shimizu, *Chem. Sci.* **2015**, *6*, 4358–4364; d) R. Pollice, M. Bot, I. J. Kobylianskii, I. G. Shenderovich, P. Chen, *J. Am. Chem. Soc.* **2017**, *139*, 13126–13140; e) J. M. Schümann, J. P. Wagner, A. K. Eckhardt, H. Quanz, P. R. Schreiner, *J. Am. Chem. Soc.* **2021**, *143*, 41–45.
[20] a) N. Becker, K. Noyes, M. Cooper, *J. Chem. Educ.* **2016**, *93*, 1713–1724; b) K. Noyes, R. L. McKay, M. Neumann, K. C. Haudek, M. M. Cooper, *J. Chem. Educ.* **2020**, *97*, 3923–3936; c) K. Noyes, M. M. Cooper, *J. Chem. Educ.* **2019**, *96*, 1821–1832.
[21] a) Y. Zhao, D. G. Truhlar, *J. Chem. Theory Comput.* **2007**, *3*, 289–300; b) Y. Zhao, D. G. Truhlar, *Acc. Chem. Res.* **2008**, *41*, 157–167; c) Y. Zhao, D. G. Truhlar, *Theor. Chem. Acc.* **2008**, *120*, 215–241; d) Y. Zhao, D. G. Truhlar, *J. Chem. Theory Comput.* **2011**, *7*, 669–676.
[22] Y. Liu, C. Zhang, Z. Liu, D. G. Truhlar, Y. Wang, X. He, *Nat. Comput. Sci.* **2022**, *3*, 48–58.
[23] a) S. N. Steinmann, C. Corminboeuf, *J. Chem. Phys.* **2011**, *134*, 044117; b) S. N. Steinmann, C. Corminboeuf, *Chimia* **2011**, *65*, 240–244; c) C. Corminboeuf, *Acc. Chem. Res.* **2014**, *47*, 3217–3224.
[24] a) A. Tkatchenko, M. Scheffler, *Phys. Rev. Lett.* **2009**, *102*, 073005; b) L. Kronik, A. Tkatchenko, *Acc. Chem. Res.* **2014**, *47*, 3208–3216; c) J. Hermann, R. A. DiStasio, A. Tkatchenko, *Chem. Rev.* **2017**, *117*, 4714–4758; d) N. Marom, A. Tkatchenko, M. Rossi, V. V. Gobre, O. Hod, M. Scheffler, L. Kronik, *J. Chem. Theory Comput.* **2011**, *7*, 3944–3951.
[25] a) S. Grimme, A. Hansen, J. G. Brandenburg, C. Bannwarth, *Chem. Rev.* **2016**, *116*, 5105–5154; b) M. Bursch, H. Neugebauer, S. Grimme, *Angew. Chem. Int. Ed.* **2019**, *58*, 11078–11087.
[26] S. Ehrlich, J. Moellmann, S. Grimme, *Acc. Chem. Res.* **2013**, *46*, 916–926.
[27] a) M. J. Allen, D. J. Tozer, *J. Chem. Phys.* **2002**, *117*, 11113; b) E. R. Johnson, A. D. Becke, *J. Chem. Phys.* **2006**, *124*, 174104; c) J. Cerny, P. Hobza, *Phys. Chem. Chem. Phys.* **2005**, *7*, 1624–1626; d) P. Jurecka, J. Cerny, P. Hobza, D. R. Salahub, *J. Comput. Chem.* **2007**, *28*, 555–569; e) J.-D. Chai, M. Head-Gordon, *J. Chem. Phys.* **2008**, *128*, 084106; f) N. Marom, A. Tkatchenko, M. Scheffler, L. Kronik, *J. Chem. Theory Comput.* **2010**, *6*, 81–90; g) O. A. Vydrov, T. Van Voorhis, *J. Chem. Phys.* **2010**, *133*, 244103-1–244103-9.
[28] a) S. Grimme, J. Antony, S. Ehrlich, H. Krieg, *J. Chem. Phys.* **2010**, *132*, 154104–154119; b) J. Klimeš, A. Michaelides, *J. Chem. Phys.* **2012**, *137*, 120901.
[29] E. R. Johnson, A. D. Becke, *J. Chem. Phys.* **2005**, *123*, 024101.
[30] a) E. Caldeweyher, C. Bannwarth, S. Grimme, *J. Chem. Phys.* **2017**, *147*, 034112; b) E. Caldeweyher, S. Ehlert, A. Hansen, H. Neugebauer, S. Spicher, C. Bannwarth, S. Grimme, *J. Chem. Phys.* **2019**, *150*, 154122.
[31] a) M. Bursch, E. Caldeweyher, A. Hansen, H. Neugebauer, S. Ehlert, S. Grimme, *Acc. Chem. Res.* **2019**, *52*, 258–266; b) E. Caldeweyher, J.-M. Mewes, S. Ehlert, S. Grimme, *Phys. Chem. Chem. Phys.* **2020**, *22*, 8499–8512.
[32] W. B. Schneider, G. Bistoni, M. Sparta, M. Saitow, C. Riplinger, A. A. Auer, F. Neese, *J. Chem. Theory Comput.* **2016**, *12*, 4778–4792.
[33] a) C. Riplinger, F. Neese, *J. Chem. Phys.* **2013**, *138*, 034106; b) D. G. Liakos, M. Sparta, M. K. Kesharwani, J. M. L. Martin, F. Neese, *J. Chem. Theory Comput.* **2015**, *11*, 1525–1539.
[34] S. F. Boys, F. Bernardi, *Mol. Phys.* **1970**, *19*, 553–566.
[35] K. Morokuma, *J. Chem. Phys.* **2003**, *55*, 1236–1244.
[36] T. M. Parker, L. A. Burns, R. M. Parrish, A. G. Ryno, C. D. Sherrill, *J. Chem. Phys.* **2014**, *140*, 094106.
[37] A. Altun, R. Izsák, G. Bistoni, *Int. J. Quantum Chem.* **2021**, *121*, e26339.
[38] G. Bistoni, A. A. Auer, F. Neese, *Chem. Eur. J.* **2017**, *23*, 865–873.
[39] Q. Lu, F. Neese, G. Bistoni, *Angew. Chem. Int. Ed.* **2018**, *57*, 4760–4764.
[40] Q. Lu, F. Neese, G. Bistoni, *Phys. Chem. Chem. Phys.* **2019**, *21*, 11569-11577, DOI: 10.1039/C9CP01309A.
[41] A. Altun, M. Saitow, F. Neese, G. Bistoni, *J. Chem. Theory Comput.* **2019**, *15*, 1616–1632.
[42] A. Altun, F. Neese, G. Bistoni, *J. Chem. Theory Comput.* **2019**, *15*, 5894–5907.
[43] K. Patkowski, *WIREs Comput. Mol. Sci.* **2020**, *10*, e1452.
[44] a) E. E. Salpeter, H. A. Bethe, *Phys. Rev.* **1951**, *84*, 1232–1242; b) S.-H. Ke, *Phys. Rev. B* **2011**, *84*, 205415.

[45] C. Holzer, W. Klopper, *J. Chem. Phys.* **2017**, *147*, 181101.
[46] M. Kodrycka, C. Holzer, W. Klopper, K. Patkowski, *J. Chem. Theory Comput.* **2019**, *15*, 5965–5986.
[47] C. Holzer, W. Klopper, *Mol. Phys.* **2017**, *115*, 2775–2781.
[48] a) K. Carter-Fenk, K. U. Lao, J. M. Herbert, *Acc. Chem. Res.* **2021**, *54*, 3679–3690; b) K. Carter-Fenk, J. M. Herbert, *Phys. Chem. Chem. Phys.* **2020**, *22*, 24870–24886; c) K. Carter-Fenk, J. M. Herbert, *Chem. Sci.* **2020**, *11*, 6758–6765.
[49] J. M. Herbert, *J. Phys. Chem. A* **2021**, *125*, 7125–7137.
[50] a) E. R. Johnson, S. Keinan, P. Mori-Sánchez, J. Contreras-García, A. J. Cohen, W. Yang, *J. Am. Chem. Soc.* **2010**, *132*, 6498–6506; b) J. Contreras-García, E. R. Johnson, S. Keinan, R. Chaudret, J.-P. Piquemal, D. N. Beratan, W. Yang, *J. Chem. Theory Comput.* **2011**, *7*, 625–632.
[51] A. Wuttke, R. A. Mata, *J. Comput. Chem.* **2017**, *38*, 15–23.
[52] R. Pollice, P. Chen, *Angew. Chem. Int. Ed.* **2019**, *58*, 9758–9769.
[53] R. Pollice, F. Fleckenstein, I. Shenderovich, P. Chen, *Angew. Chem. Int. Ed.* **2019**, *58*, 14281–14288.
[54] a) I. K. Mati, S. L. Cockroft, *Chem. Soc. Rev.* **2010**, *39*, 4195–4205; b) M. A. Strauss, H. A. Wegner, *Eur. J. Org. Chem.* **2019**, 295–302; c) M. Strauss, H. A. Wegner, *Angew. Chem. Int. Ed.* **2019**, *58*, 18552–18556.
[55] T. Grawe, T. Schrader, R. Zadmard, A. Kraft, *J. Org. Chem.* **2002**, *67*, 3755–3763.
[56] A. H. Heindl, R. C. Wende, H. A. Wegner, *Beilstein J. Org. Chem.* **2018**, *14*, 1238–1243.
[57] L. Yang, C. Adam, G. S. Nichol, S. L. Cockroft, *Nat. Chem.* **2013**, *5*, 1006–1010.
[58] D. Van Craen, W. H. Rath, M. Huth, L. Kemp, C. Räuber, J. M. Wollschläger, C. A. Schalley, A. Valkonen, K. Rissanen, M. Albrecht, *J. Am. Chem. Soc.* **2017**, *139*, 16959–16966.
[59] E.-i. Kim, S. Paliwal, C. S. Wilcox, *J. Am. Chem. Soc.* **1998**, *120*, 11192–11193.
[60] a) C. Adam, L. Yang, S. L. Cockroft, *Angew. Chem. Int. Ed.* **2015**, *54*, 1164–1167; b) L. Yang, C. Adam, S. L. Cockroft, *J. Am. Chem. Soc.* **2015**, *137*, 10084–10087.
[61] S. Otto, *Chem. Sci.* **2013**, *4*, 2953–2959.
[62] W. R. Carroll, P. Pellechia, K. D. Shimizu, *Org. Lett.* **2008**, *10*, 3547–3550.
[63] J. Hwang, P. Li, W. R. Carroll, M. D. Smith, P. J. Pellechia, K. D. Shimizu, *J. Am. Chem. Soc.* **2014**, *136*, 14060–14067.
[64] P. Li, E. C. Vic, K. D. Shimizu, *Acc. Chem. Res.* **2020**, *53*, 2705–2714.
[65] C. D. Zeinalipour-Yazdi, D. P. Pullman, *J. Phys. Chem. B* **2006**, *110*, 24260–24265.
[66] J. Hwang, P. Li, M. D. Smith, K. D. Shimizu, *Angew. Chem. Int. Ed.* **2016**, *55*, 8086–8089.
[67] A. V. Marenich, C. J. Cramer, D. G. Truhlar, *J. Phys. Chem. B* **2009**, *113*, 6378–6396.
[68] F. Eckert, A. Klamt, *AIChE J.* **2002**, *48*, 369–385.
[69] M. Schlottmann, D. Van Craen, J. Baums, I. Funes-Ardoiz, C. Wiederhold, I. M. Oppel, M. Albrecht, *Inorg. Chem.* **2020**, *59*, 1758–1762.
[70] M. H. Lyttle, A. Streitwieser Jr, R. Q. Kluttz, *J. Am. Chem. Soc.* **1981**, *103*, 3232–3233.
[71] L. A. Paquette, G. J. Hefferon, R. Samodral, Y. Hanzawa, *J. Org. Chem.* **1983**, *48*, 1262–1266.
[72] a) N. L. Allinger, M. Frierson, F. A. Van-Catledge, *J. Am. Chem. Soc.* **1982**, *104*, 4592–4593; b) C. Tosi, *J. Comput. Chem.* **1984**, *5*, 248–251.
[73] M. J. Miller, M. H. Lyttle, A. Streitwieser Jr, *J. Org. Chem.* **1981**, *46*, 1977–1984.
[74] J. E. Anderson, P. A. Kirsch, *J. Chem. Soc. Perkin Trans. 2* **1992**, 1951–1957.
[75] H. F. König, L. Rummel, H. Hausmann, J. Becker, J. M. Schümann, P. R. Schreiner, *J. Org. Chem.* **2022**, *87*, 4670–4679.
[76] a) E. L. Eliel, H. Satici, *J. Org. Chem.* **1994**, *59*, 688–689; b) C. H. Marzabadi, J. E. Anderson, J. Gonzalez-Outeirino, P. R. J. Gaffney, C. G. H. White, D. A. Tocher, L. J. Todaro, *J. Am. Chem. Soc.* **2003**, *125*, 15163–15173; c) E. Solel, M. Ruth, P. R. Schreiner, *J. Am. Chem. Soc.* **2021**, *143*, 20837–20848.
[77] S. Nobujiro, T. Naohide, Y. Sigefumi, I. Takahiko, *Chem. Lett.* **1993**, *22*, 1807–1810.
[78] C. A. Tolman, *Chem. Rev.* **1977**, *77*, 313–348.
[79] H. F. König, H. Hausmann, P. R. Schreiner, *J. Am. Chem. Soc.* **2022**, *144*, 16965–16973.
[80] a) F. M. Wilming, B. Marazzi, P. P. Debes, J. Becker, P. R. Schreiner, *J. Org. Chem.* **2023**, *88*, 1024–1035; b) F. M. Wilming, J. Becker, P. R. Schreiner, *J. Org. Chem.* **2022**, *87*, 1874–1878.
[81] a) M. Minabe, A. Yamazaki, T. Imai, T. Takanezawa, M. Karikomi, *Bull. Chem. Soc. Jpn.* **2006**, *79*, 1758–1765; b) M. Minabe, T. Oba, M. Tanaka, K. Kanno, M. Tsubota, *Chem. Lett.* **2000**, *29*, 498–499.
[82] J. Gorges, S. Grimme, A. Hansen, P. Pracht, *Phys. Chem. Chem. Phys.* **2022**, *24*, 12249–12259.
[83] a) A. Tsybizova, L. Fritsche, V. Gorbachev, L. Miloglyadova, P. Chen, *J. Chem. Phys.* **2019**, *151*, 234304; b) V. Gorbachev, A. Tsybizova, L. Miloglyadova, P. Chen, *J. Am. Chem. Soc.* **2022**, *144*, 9007–9022.
[84] a) C. A. Hunter, *Chem. Sci.* **2013**, *4*, 834–848; b) C. Bravin, J. A. Piękoś, G. Licini, C. A. Hunter, C. Zonta, *Angew. Chem. Int. Ed.* **2021**, *60*, 23871–23877.
[85] K. Nakamura, K. N. Houk, *Org. Lett.* **1999**, *1*, 2049–2051.
[86] a) D. Chandler, *Nature* **2005**, *437*, 640–647; b) A. Elmi, S. L. Cockroft, *Acc. Chem. Res.* **2021**, *54*, 92–103.
[87] R. Pollice, P. Chen, *J. Am. Chem. Soc.* **2019**, *141*, 3489–3506.
[88] M. A. Strauss, H. A. Wegner, *Angew. Chem. Int. Ed.* **2021**, *60*, 779–786.
[89] D. Schatz, A. Kunz, A. R. Raab, H. A. Wegner, *Synlett* **2023**, *34*, 1153–1158.
[90] K. Szalewicz, *WIREs Comput. Mol. Sci.* **2012**, *2*, 254–272.
[91] J. M. Schümann, L. Ochmann, J. Becker, A. Altun, I. Harden, G. Bistoni, P. R. Schreiner, *J. Am. Chem. Soc.* **2023**, *145*, 2093–2097.
[92] M. Gomberg, *J. Am. Chem. Soc.* **1900**, *22*, 757–771.
[93] H. Lankamp, W. T. Nauta, C. MacLean, *Tetrahedron Lett.* **1968**, *9*, 249–254.
[94] a) W. D. Hounshell, D. A. Dougherty, J. P. Hummel, K. Mislow, *J. Am. Chem. Soc.* **1977**, *99*, 1916–1924; b) E. Osawa, Y. Onuki, K. Mislow, *J. Am. Chem. Soc.* **1981**, *103*, 7475–7479.
[95] a) M. Stein, W. Winter, A. Rieker, *Angew. Chem. Int. Ed. Engl.* **1978**, *17*, 692–694; b) B. Kahr, D. van Engen, K. Mislow, *J. Am. Chem. Soc.* **1986**, *108*, 8305–8307; c) N. Yannoni, B. Kahr, K. Mislow, *J. Am. Chem. Soc.* **1988**, *110*, 6670–6672.
[96] a) S. Rösel, H. Quanz, C. Logemann, J. Becker, E. Mossou, L. Canadillas-Delgado, E. Caldeweyher, S. Grimme, P. R. Schreiner, *J. Am. Chem. Soc.* **2017**, *139*, 7428–7431; b) D. Maué, P. Strebert, D. Bernhard, S. Rösel, P. R. Schreiner, M. Gerhards, *Angew. Chem. Int. Ed.* **2021**, *60*, 11305–11309.
[97] A. A. Fokin, L. V. Chernish, P. A. Gunchenko, E. Y. Tikhonchuk, H. Hausmann, M. Serafin, J. E. P. Dahl, R. M. K. Carlson, P. R. Schreiner, *J. Am. Chem. Soc.* **2012**, *134*, 13641–13650.
[98] A. A. Fokin, T. S. Zhuk, S. Blomeyer, C. Pérez, L. V. Chernish, A. Pashenko, J. Antony, Y. V. Vishnevskiy, R. J. F. Berger, S. Grimme, C. Logemann, M. Schnell, N. W. Mitzel, P. R. Schreiner, *J. Am. Chem. Soc.* **2017**, *139*, 16696–16707.

[99] Y. Ishigaki, T. Shimajiri, Y. Kawakami, S. Kawaguchi, Y. Hayashi, K. Hada, T. Suzuki, *Synlett* **2023**, *34*, 1147–1152.

[100] F. Holtrop, C. Helling, M. Lutz, K. Van Leest, B. de Bruin, C. Slootweg, *Synlett* **2023**, *34*, 1122–1128.

[101] a) C. Medcraft, S. Zinn, M. Schnell, A. Poblotzki, J. Altnöder, M. Heger, M. A. Suhm, D. Bernhard, A. Stamm, F. Dietrich, M. Gerhards, *Phys. Chem. Chem. Phys.* **2016**, *18*, 25975–25983; b) D. Bernhard, C. Holzer, F. Dietrich, A. Stamm, W. Klopper, M. Gerhards, *ChemPhysChem* **2017**, *18*, 3634–3641; c) D. Bernhard, F. Dietrich, M. Fatima, C. Perez, A. Poblotzki, G. Jansen, M. A. Suhm, M. Schnell, M. Gerhards, *Phys. Chem. Chem. Phys.* **2017**, *19*, 18076–18088; d) F. Dietrich, D. Bernhard, M. Fatima, C. Pérez, M. Schnell, M. Gerhards, *Angew. Chem. Int. Ed.* **2018**, *57*, 9534–9537; e) D. Bernhard, F. Dietrich, M. Fatima, C. Perez, H. C. Gottschalk, A. Wuttke, R. A. Mata, M. A. Suhm, M. Schnell, M. Gerhards, *Beilstein J. Org. Chem.* **2018**, *14*, 1642–1654.

[102] D. Bernhard, M. Fatima, A. Poblotzki, A. L. Steber, C. Pérez, M. A. Suhm, M. Schnell, M. Gerhards, *Phys. Chem. Chem. Phys.* **2019**, *21*, 16032–16046.

[103] M. Fatima, A. L. Steber, A. Poblotzki, C. Pérez, S. Zinn, M. Schnell, *Angew. Chem. Int. Ed.* **2019**, *58*, 3108–3113.

[104] a) C. Pérez, J. C. López, S. Blanco, M. Schnell, *J. Phys. Chem. Lett.* **2016**, *7*, 4053–4058; b) C. Pérez, A. Krin, A. L. Steber, J. C. López, Z. Kisiel, M. Schnell, *J. Phys. Chem. Lett.* **2016**, *7*, 154–160; c) S. Zinn, C. Medcraft, T. Betz, M. Schnell, *Angew. Chem. Int. Ed.* **2016**, *55*, 5975–5980; d) S. R. Domingos, C. Pérez, M. Schnell, *J. Chem. Phys.* **2016**, *145*, 161103.

[105] M. M. Quesada Moreno, P. Pinacho, C. Pérez, M. Šekutor, P. R. Schreiner, M. Schnell, *Chem. Eur. J.* **2020**, *26*, 10817–10825.

[106] M. M. Quesada-Moreno, P. Pinacho, C. Pérez, M. Šekutor, P. R. Schreiner, M. Schnell, *Chem. Eur. J.* **2021**, *27*, 6198–6203.

[107] A. Poblotzki, H. C. Gottschalk, M. A. Suhm, *J. Phys. Chem. Lett.* **2017**, 5656–5665.

[108] B. Hartwig, M. Lange, A. Poblotzki, R. Medel, A. Zehnacker, M. A. Suhm, *Phys. Chem. Chem. Phys.* **2020**, *22*, 1122–1136.

[109] a) R. Medel, M. A. Suhm, *Phys. Chem. Chem. Phys.* **2020**, *22*, 25538–25551; b) R. Medel, A. Camiruaga, R. T. Saragi, P. Pinacho, C. Pérez, M. Schnell, A. Lesarri, M. A. Suhm, J. A. Fernández, *Phys. Chem. Chem. Phys.* **2021**, *23*, 23610–23624.

[110] T. Forsting, H. C. Gottschalk, B. Hartwig, M. Mons, M. A. Suhm, *Phys. Chem. Chem. Phys.* **2017**, *19*, 10727–10737.

[111] a) M. Heger, J. Altnöder, A. Poblotzki, M. A. Suhm, *Phys. Chem. Chem. Phys.* **2015**, *17*, 13045–13052; b) A. Poblotzki, J. Altnöder, M. A. Suhm, *Phys. Chem. Chem. Phys.* **2016**, *18*, 27265–27271; c) H. C. Gottschalk, J. Altnöder, M. Heger, M. A. Suhm, *Angew. Chem. Int. Ed.* **2016**, *55*, 1921–1924; d) C. Zimmermann, H. C. Gottschalk, M. A. Suhm, *Phys. Chem. Chem. Phys.* **2020**, *22*, 2870–2877; e) C. Zimmermann, T. L. Fischer, M. A. Suhm, *Molecules* **2020**, *25(21)*, 5059, DOI: 10.3390/molecules25215095; f) C. Zimmermann, M. Lange, M. A. Suhm, *Molecules* **2021**, *26*, 4883.

[112] J. P. Wagner, P. R. Schreiner, *J. Chem. Theory Comput.* **2016**, *12*, 231–237.

[113] C. F. Matta, J. Hernández-Trujillo, T.-H. Tang, R. F. W. Bader, *Chem. Eur. J.* **2003**, *9*, 1940–1951.

[114] M.-L. Y. Riu, G. Bistoni, C. C. Cummins, *J. Phys. Chem. A* **2021**, *125*, 6151–6157.

[115] M.-L. Y. Riu, R. L. Jones, W. J. Transue, P. Müller, C. C. Cummins, *Sci. Adv.* **2020**, *6*, eaaz3168.

[116] a) S. Winstein, N. J. Holness, *J. Am. Chem. Soc.* **1955**, *77*, 5562–5578; b) F. R. Jensen, C. H. Bushweller, B. H. Beck, *J. Am. Chem. Soc.* **1969**, *91*, 344–351.

[117] V. Fasano, A. W. McFord, C. P. Butts, B. S. L. Collins, N. Fey, R. W. Alder, V. K. Aggarwal, *Angew. Chem. Int. Ed.* **2020**, *59*, 22403–22407.

[118] a) H.-J. Schneider, *Acc. Chem. Res.* **2015**, *48*, 1815–1822; b) E. Solel, M. Ruth, P. R. Schreiner, *J. Org. Chem.* **2021**, *86*, 7701–7713.

[119] a) R. R. Knowles, E. N. Jacobsen, *Proc. Natl. Acad. Sci. USA* **2010**, *107*, 20678–20685; b) K. T. Mahmudov, A. V. Gurbanov, F. I. Guseinov, M. F. C. Guedes da Silva, *Coord. Chem. Rev.* **2019**, *387*, 32–46; c) F. Holtrop, K. W. Visscher, A. R. Jupp, J. C. Slootweg, *Adv. Phys. Org. Chem.* **2020**, 119–141; d) A. Fanourakis, P. J. Docherty, P. Chuentragool, R. J. Phipps, *ACS Catal.* **2020**, *10*, 10672–10714; e) K. L. Mears, P. P. Power, *Acc. Chem. Res.* **2022**, *55*, 1337–1348.

[120] A. J. Neel, M. J. Hilton, M. S. Sigman, F. D. Toste, *Nature* **2017**, *543*, 637–646.

[121] a) A. Wittkopp, Dissertation, University Göttingen (Germany), **2001**; b) A. Wittkopp, P. R. Schreiner, in *The Chemistry of Dienes and Polyenes, Vol. 2* (Ed.: Z. Rappoport), John Wiley & Sons, Ltd, Hoboken, **2000**, pp. 1029–1088; c) A. Wittkopp, Diploma Thesis thesis, University of Göttingen (Germany), **1997**; d) P. R. Schreiner, A. Wittkopp, *Org. Lett.* **2002**, *4*, 217–220; e) K. M. Lippert, K. Hof, D. Gerbig, D. Ley, H. Hausmann, S. Guenther, P. R. Schreiner, *Eur. J. Org. Chem.* **2012**, 5919–5927.

[122] L. Rummel, M. H. J. Domanski, H. Hausmann, J. Becker, P. R. Schreiner, *Angew. Chem. Int. Ed.* **2022**, *61*, e202204393.

[123] a) S. Singha, M. Buchsteiner, G. Bistoni, R. Goddard, A. Fürstner, *J. Am. Chem. Soc.* **2021**, *143*, 5666–5673; b) M. Buchsteiner, S. Singha, J. Decaens, A. Fürstner, *Angew. Chem. Int. Ed.* **2022**, *61*, e202212546.

[124] L. P. Wolters, R. Koekkoek, F. M. Bickelhaupt, *ACS Catal.* **2015**, *5*, 5766–5775.

[125] I. Harden, F. Neese, G. Bistoni, *Chem. Sci.* **2022**, *13*, 8848–8859, DOI: 10.1039/D2SC02274E.

[126] N. Tsuji, J. L. Kennemur, T. Buyck, S. Lee, S. Prévost, P. S. J. Kaib, D. Bykov, C. Farès, B. List, *Science* **2018**, *359*, 1501–1505.

[127] a) R. C. Wende, A. Seitz, D. Niedek, S. M. M. Schuler, C. Hofmann, J. Becker, P. R. Schreiner, *Angew. Chem. Int. Ed.* **2016**, *55*, 2719–2723; b) E. Procházková, A. Kolmer, J. Ilgen, M. Schwab, L. Kaltschnee, M. Fredersdorf, V. Schmidts, R. C. Wende, P. R. Schreiner, C. M. Thiele, *Angew. Chem. Int. Ed.* **2016**, *55*, 15754–15759; c) J. Miró, T. Gensch, M. Ellwart, S.-J. Han, H.-H. Lin, M. S. Sigman, F. D. Toste, *J. Am. Chem. Soc.* **2020**, *142*, 6390–6399.

[128] a) T. Hansen, X. Sun, M. Dalla Tiezza, W. J. van Zeist, J. N. P. van Stralen, D. P. Geerke, L. P. Wolters, J. Poater, T. A. Hamlin, F. M. Bickelhaupt, *Chem. Eur. J.* **2022**, e202201093; b) R. Hoffmann, C. C. Levin, R. A. Moss, *J. Am. Chem. Soc.* **1973**, *95*, 629–631; c) G. Gryn'ova, C. Corminboeuf, *Beilstein J. Org. Chem.* **2018**, *14*, 1482–1490; d) R. R. Sauers, *J. Chem. Educ.* **1996**, *73*, 114.

[129] M. Marin-Luna, B. Polloth, F. Zott, H. Zipse, *Chem. Sci.* **2018**, *9*, 6509–6515.

[130] B. Pölloth, M. P. Sibi, H. Zipse, *Angew. Chem. Int. Ed.* **2021**, *60*, 774–778.

[131] E. J. Corey, R. K. Bakshi, S. Shibata, C. P. Chen, V. K. Singh, *J. Am. Chem. Soc.* **1987**, *109*, 7925–7926.

[132] a) E. J. Corey, J. O. Link, R. K. Bakshi, *Tetrahedron Lett.* **1992**, *33*, 7107–7110; b) E. J. Corey, C. J. Helal, *Tetrahedron Lett.* **1995**, *36*, 9153–9156; c) E. J. Corey, C. J. Helal, *Angew. Chem. Int. Ed.* **1998**, *37*, 1986–2012.

[133] S. Hanlon, *Biochem. Biophys. Res. Commun.* **1966**, *23*, 861–867.

[134] a) J. Vondrášek, T. Kubař, F. E. Jenney Jr, M. W. W. Adams, M. Kožíšek, J. Černý, V. Sklenář, P. Hobza, *Chem. Eur. J.*

2007, *13*, 9022–9027; b) R. Sedlák, P. Jurečka, P. Hobza, *J. Chem. Phys.* **2007**, *127*, 075104; c) J. Šponer, K. E. Riley, P. Hobza, *Phys. Chem. Chem. Phys.* **2008**, *10*, 2595–2610; d) O. A. Stasyuk, D. Jakubec, J. Vondrášek, P. Hobza, *J. Chem. Theory Comput.* **2017**, *13*, 877–885.
[135] A. Altun, M. Garcia-Ratés, F. Neese, G. Bistoni, *Chem. Sci.* **2021**, *12*, 12785–12793.
[136] a) C. E. Müller, P. R. Schreiner, *Angew. Chem. Int. Ed.* **2011**, *50*, 6012–6042; b) C. E. Müller, L. Wanka, K. Jewell, P. R. Schreiner, *Angew. Chem. Int. Ed.* **2008**, *47*, 6180–6183.
[137] E. A. C. Davie, S. M. Mennen, Y. J. Xu, S. J. Miller, *Chem. Rev.* **2007**, *107*, 5759–5812.
[138] C. E. Müller, D. Zell, R. Hrdina, R. C. Wende, L. Wanka, S. M. M. Schuler, P. R. Schreiner, *J. Org. Chem.* **2013**, *78*, 8465–8484.
[139] a) A. Seitz, R. Wende, P. R. Schreiner, *Chem. Eur. J.* **2023**, *29*, e202203002; b) A. Seitz, R. C. Wende, E. Roesner, D. Niedek, C. Topp, A. C. Colgan, E. M. McGarrigle, P. R. Schreiner, *J. Org. Chem.* **2021**, *86*, 3907–3922.
[140] J. Gramüller, M. Franta, R. M. Gschwind, *J. Am. Chem. Soc.* **2022**, *144*, 19861–19871.
[141] A. C. Colgan, R. S. J. Proctor, D. C. Gibson, P. Chuentragool, A. S. K. Lahdenperä, K. Ermanis, R. J. Phipps, *Angew. Chem. Int. Ed.* **2022**, *61*, e202200266.
[142] a) J. Tu, D. Svatunek, S. Parvez, A. C. Liu, B. J. Levandowski, H. J. Eckvahl, R. T. Peterson, K. N. Houk, R. M. Franzini, *Angew. Chem. Int. Ed.* **2019**, *58*, 9043–9048; b) T. Deb, R. M. Franzini, *Synlett* **2020**, *31*, 938–944.
[143] L. Pauling, *Nature* **1948**, *161*, 707–709.
[144] A. A. Kroeger, J. F. Hooper, A. Karton, *ChemPhysChem* **2020**, *21*, 1675–1681.
[145] A. Karton, *J. Phys. Chem. A* **2020**, *124*, 6977–6985.
[146] R. Guo, S. Adak, P. Bellotti, X. Gao, W. W. Smith, S. N. Le, J. Ma, K. N. Houk, F. Glorius, S. Chen, M. K. Brown, *J. Am. Chem. Soc.* **2022**, *144*, 17680–17691.
[147] F. H. John, *Organotransition metal chemistry: from bonding to catalysis*, University Science Books, **2010**.
[148] a) N. Fey, *Dalton Trans.* **2010**, *39*, 296–310; b) D. J. Nelson, S. P. Nolan, *Chem. Soc. Rev.* **2013**, *42*, 6723.
[149] M. Raynal, P. Ballester, A. Vidal-Ferran, P. W. N. M. van Leeuwen, *Chem. Soc. Rev.* **2014**, *43*, 1660–1733.
[150] a) R. Noyori, *Angew. Chem. Int. Ed.* **2002**, *41*, 2008–2022; b) C. Valente, S. Çalimsiz, K. H. Hoi, D. Mallik, M. Sayah, M. G. Organ, *Angew. Chem. Int. Ed.* **2012**, *51*, 3314–3332; c) G. Lu, C. Fang, T. Xu, G. Dong, P. Liu, *J. Am. Chem. Soc.* **2015**, *137*, 8274–8283.
[151] I. Kalvet, K. Deckers, I. Funes-Ardoiz, G. Magnin, T. Sperger, M. Kremer, F. Schoenebeck, *Angew. Chem. Int. Ed.* **2020**, *59*, 7721–7725.
[152] Y. Zhao, D. G. Truhlar, *Org. Lett.* **2007**, *9*, 1967–1970.
[153] M. Marin-Luna, P. Patschinski, H. Zipse, *Chem. Eur. J.* **2018**, *24*, 15052–15058.
[154] S. Sakai, A. Fujioka, K. Imai, K. Uchiyama, Y. Shimizu, K. Higashida, M. Sawamura, *Adv. Synth. Catal.* **2022**, *364*, 2333–2339.
[155] M. C. Schwarzer, A. Fujioka, T. Ishii, H. Ohmiya, S. Mori, M. Sawamura, *Chem. Sci.* **2018**, *9*, 3484–3493.
[156] D. Zell, M. Bursch, V. Müller, S. Grimme, L. Ackermann, *Angew. Chem. Int. Ed.* **2017**, *56*, 10378–10382.
[157] E. Detmar, V. Müller, D. Zell, L. Ackermann, M. Breugst, *Beilstein J. Org. Chem.* **2018**, *14*, 1537–1545.
[158] T. H. Meyer, W. Liu, M. Feldt, A. Wuttke, R. A. Mata, L. Ackermann, *Chem. Eur. J.* **2017**, *23*, 5443–5447.
[159] a) D. Ghorai, V. Müller, H. Keil, D. Stalke, G. Zanoni, B. A. Tkachenko, P. R. Schreiner, L. Ackermann, *Adv. Synth. Catal.* **2017**, *359*, 3137–3141; b) K. Reinhardt, S. Koller, P. Klein, C. Lossin, J. Gatzka, P. J. Altmann, A. Pöthig, L. Hintermann, *Organometallics* **2022**, *41*, 1–19.
[160] T. G. Saint-Denis, N. Y. S. Lam, N. Chekshin, P. F. Richardson, J. S. Chen, J. Elleraas, K. D. Hesp, D. C. Schmitt, Y. Lian, C. W. Huh, J.-Q. Yu, *ACS Catal.* **2021**, *11*, 9738–9753.
[161] B. G. Hejna, J. M. Ganley, H. Shao, H. Tian, J. D. Ellefsen, N. J. Fastuca, K. N. Houk, S. J. Miller, R. R. Knowles, *J. Am. Chem. Soc.* **2023**, *145*, 16118–16129.
[162] a) A. Changotra, B. Bhaskararao, C. M. Hadad, R. B. Sunoj, *J. Am. Chem. Soc.* **2020**, *142*, 9612–9624; b) H. Xu, B. Li, Z. Liu, Y. Dang, *ACS Catal.* **2021**, *11*, 9008–9021; c) B. Li, H. Xu, Y. Dang, K. N. Houk, *J. Am. Chem. Soc.* **2022**, *144*, 1971–1985.
[163] S. Meninno, M. Meazza, J. W. Yang, T. Tejero, P. Merino, R. Rios, *Chem. Eur. J.* **2019**, *25*, 7623–7627.
[164] S. M. Maley, R. Steagall, G. R. Lief, R. M. Buck, Q. Yang, O. L. Sydora, S. M. Bischof, D. H. Ess, *Organometallics* **2022**, *41*, 581–593.
[165] a) M. Paul, M. Breugst, J. M. Neudorfl, R. B. Sunoj, A. Berkessel, *J. Am. Chem. Soc.* **2016**, *138*, 5044–5051; b) V. R. Yatham, W. Harnying, D. Kootz, J.-M. Neudörfl, N. E. Schlörer, A. Berkessel, *J. Am. Chem. Soc.* **2016**, *138*, 2670–2677; c) M. Paul, P. Sudkaow, A. Wessels, N. E. Schlorer, J. M. Neudorfl, A. Berkessel, *Angew. Chem. Int. Ed.* **2018**, *57*, 8310–8315; d) M. Paul, J.-M. Neudörfl, A. Berkessel, *Angew. Chem. Int. Ed.* **2019**, *58*, 10596–10600; e) W. Harnying, J.-M. Neudörfl, A. Berkessel, *Org. Lett.* **2020**, *22*, 386–390; f) W. Harnying, P. Sudkaow, A. Biswas, A. Berkessel, *Angew. Chem. Int. Ed.* **2021**, *60*, 19631–19636, DOI: 10.1002/anie.202104712.
[166] L. P. Ho, A. Nasr, P. G. Jones, A. Altun, F. Neese, G. Bistoni, M. Tamm, *Chem. Eur. J.* **2018**, *24*, 18922–18932.
[167] P. Śliwa, M. P. Mitoraj, F. Sagan, J. Handzlik, *J. Mol. Model.* **2019**, *25*, 331.
[168] A. Hamza, D. Moock, C. Schlepphorst, J. Schneidewind, W. Baumann, F. Glorius, *Chem. Sci.* **2022**, *13*, 985–995.
[169] D. E. Koshland, *Proc. Natl. Acad. Sci. USA* **1958**, *44*, 98.
[170] D. Yepes, F. Neese, B. List, G. Bistoni, *J. Am. Chem. Soc.* **2020**, *142*, 3613–3625.
[171] N. I. Saper, A. Ohgi, D. W. Small, K. Semba, Y. Nakao, J. F. Hartwig, *Nat. Chem.* **2020**, *12*, 276–283.
[172] D. Baek, H. Ryu, J. Y. Ryu, J. Lee, B. M. Stoltz, S. Hong, *Chem. Sci.* **2020**, *11*, 4602–4607.
[173] L. R. Andreola, S. E. Wheeler, *Org. Chem. Front.* **2022**, *9*, 3027–3033.

Manuscript received: October 29, 2023
Accepted manuscript online: December 5, 2023
Version of record online: January 4, 2024